Polycyclic aromatic hydrocarbons influence naïve $CD4^+$ T cell differentiation

By
2019

Amanda J. Dunbar
B.A., University of Minnesota, Morris 2011

Submitted to the graduate degree program in Molecular Biosciences and the Graduate Faculty of the University of Kansas in partial fulfillment of the requirements for the degree of Master of Arts.

Chair: Dr. Stephen H. Benedict

Dr. Susan Egan

Dr. David Davido

Date Defended: September 9, 2019

The thesis committee for Amanda J. Dunbar certifies that this is the approved version of the following thesis:

Polycyclic aromatic hydrocarbons influence naïve CD4$^+$ T cell differentiation

Chair: Dr. Stephen H. Benedict

Date Approved: September 9, 2019

Abstract

$CD4^+$ T cells are essential for the effective functioning and appropriate regulation of the immune system. Antigen-naïve T cells require two distinct costimulatory signals to activate and differentiate into effector and memory T cells which can respond to antigen and direct the immune response. The first signal is through cognate antigen presented in major histocompatibility class II on an antigen-presenting cell binding to the T cell receptor. The second signal is the interaction of a costimulatory receptor on the T cell with a counter-receptor expressed on the antigen-presenting cell. This work focuses on the costimulatory receptors CD28, the classic T cell costimulatory molecule, and intercellular adhesion molecule-1 (ICAM-1). ICAM-1 functions in adhesion and extravasation during inflammation, and our lab has previously published that ICAM-1 can function as a T cell second signal for activation.

Polycyclic aromatic hydrocarbons (PAHs) are ubiquitous environmental contaminants which have been shown by many other investigators to have diverse effects on human health including the immune system. In the present work, we examined the consequences of exposure to two PAHs during naïve T cell costimulation. Bisphenol A, a widely used plasticizer and component of epoxy resins, was found to weakly promote naïve T cell proliferation during ICAM-1 costimulation but not in CD28 costimulation and did not perturb effector and memory cell differentiation in either costimulation. Pyrene, a product of incomplete combustion of organic materials, enhanced proliferation of naïve T cells in both ICAM-1 and CD28 costimulations and inhibited effector and memory cell differentiation in both costimulations.

We also compared the differentiation of naïve T cells isolated using StemSep and EasySep naïve CD4+ T cell isolation kits upon being informed by StemCell, the manufacturer of

the kits, that StemSep was being discontinued in favor of EasySep. In contrast to StemSep naïve T cells, with which we have published previously, EasySep-purified naïve T cells did not differentiate in response to costimulation through ICAM-1 or CD28 without addition of exogenous cytokines and had dramatically increased cell death. We showed that inclusion of CD25 antibody in the EasySep negative selection antibody cocktail was partially responsible for the observed loss of differentiation and viability. Likewise, the EasySep magnetic beads were partially at fault for observed failure to differentiate and loss of viability in EasySep naïve T cells. This result also suggested an important role for the $CD25^{lo}$ population of naïve T cells in the ability of the cells to differentiate, which is in keeping with the published literature.

Acknowledgements

The list of people I'd like to thank for making it this far is incredibly long, but here are the overachievers.

Steve, I am very grateful for all your help over the years, including but not limited to putting up with all my brilliant, snarky comments, large quantities of Post-It notes stuck to all the lab surfaces, and creative experiments involving hair color. Most especially, thank you for not giving up on me in spite of it all.

Anuja, my experience in this lab would not have been the same without you. Thank you so much for helping when I was sick (which was often) and for listening and for your friendship. You are responsible for a great deal of the preservation of my sanity during this crazy journey. I am so glad I got to know you!

Daddy, Zack, and Mom: thank you for believing in me, always. Thank you for nurturing my love of biology, for supporting my dreams, and for helping me remember what is really important and, most particularly, what is not.

My "babies", Rosie, Crick, George, Lucy, and Fred. Thank you for your unconditional love, for always knowing when I need snuggles, and for never letting me forget about dinnertime.

And finally . . .

Corwin. I can say with complete sincerity that I would not be here today without your love and your support. You make me happy every single day, and every single day I am so grateful for our little family. Thank you for EVERYTHING. Everything encompasses helping me figure out how to use crutches, listening to a million complaints about work and my hands and leaving your socks on the floor, listening to elaborate explanations involving flow cytometry and lasers, being okay with eating a lot of microwave dinners, traveling to the "wasteland" to visit my family, watching Planet Earth over and over, etc. Most of all though, thank you for making each day fun, for staying through all the bad times as well as the good, and for believing in me when I wasn't sure I believed in myself. I am a better person for having known you, and I can't wait to see what the future brings. Love you!

Table of contents

List of tables

List of figures

Chapter 1. Introduction

The immune system. The immune system has an innate branch and an adaptive branch. The innate branch is nonspecific and includes barrier defenses such as skin and mucosa. The adaptive branch recognizes and can remember specific threats. The adaptive branch consists of B cells, T cells, and antigen-presenting cells (APCs). B cells develop in the bone marrow and produce antibodies that bind to specific antigens and are responsible for humoral immunity. Pre-T cells arise in the bone marrow and migrate to the thymus, where they develop into T cells, undergoing a selection process based on self/nonself recognition through the newly expressed T cell receptor (TCR).

TCR/CD3 complex. The TCR is a specialized membrane receptor which can interact with only one specific, unique antigen (referred to as the cognate antigen). The TCR has two subunits, TCRα and TCRβ or TCRγ and TCRδ. The majority of T cells in the blood express TCRαβ, while cells bearing γδ TCRs make up less than 5% of T cells in the blood in humans and mice (1). However, most of the skin-resident T cells are γδ T cells. γδ T cells primarily respond to lipid antigens presented in CD1, while αβ T cells respond to peptide antigens presented within the major histocompatibility complex (MHC, known as HLA in humans).

The TCR is always co-expressed with several accessory proteins known as CD3. The CD3 complex includes the εδ, γε, and ζζ dimers as well as TCRαβ or TCRγδ. CD3 is required to stabilize the TCR complex and to transduce signals across the membrane, as the TCR itself has extremely short cytoplasmic tails which cannot signal. CD3 signals via immunoreceptor tyrosine-based activation motifs (ITAMs) which consist of a YxxL/Ix_{6-8}YxxL/I sequence. CD3 δ, ε, and γ each have one ITAM, while the ζ chains each possess 3 ITAMs, resulting in a total of 10 ITAMs associated with each TCR complex. When the TCR binds to its cognate antigen, the

tyrosine residues in the ITAMs are quickly phosphorylated by kinases such as Lck, Fyn, ZAP-70, Syk, Itk, and others. The phosphorylated ITAMs become docking sites for SH2 domain-containing proteins, which propogate the signal downstream.

Mature T cells express either of the TCRαβ co-receptors CD8 or CD4. $CD8^+$ T cells are also known as cytotoxic T cells because they recognize specific antigens presented in MHC class I and, when stimulated by cytokines, can kill target cells via the granzyme and perforin pathways. $CD8^+$ T cells primarily target virus-infected cells. $CD4^+$ T cells represent T helper cells or T regulatory cells. $CD4^+$ T cells recognize antigen presented in MHC class II on APCs and produce cytokines which can direct the activity of other cells in an immune response.

Maturation of T cells in the thymus is considered primary lymphoid development. 95% of developing T cells die during this process of thymic selection. A T cell that survives thymic selection and leaves the thymus but has not yet encountered its cognate antigen is referred to as "naïve". Naïve $CD4^+$ T cells are classically defined as having the phenotype $CD45RA^+$ $RO^{(-)}$ $CD11a^+$ $CD27^{lo}$ $CD62L^+$ $CCR7^+$ (2-3), though recent studies indicate they are also $CD25^{lo}$ (4-5). Upon binding to the specific antigen that corresponds to a given cell's TCR, the cell divides several times and undergoes a differentiation process. The factors that control the phenotypic outcome of naïve T cell differentiation are not entirely understood, although they appear to depend on the local cytokine milieu as well as specific receptor-mediated cell:cell contacts. This process is known as secondary lymphoid differentiation and occurs in the lymphoid follicles of the lymph nodes, spleen, and mucosal-associated lymphoid tissue. During this process, the cell becomes activated is referred to as a lymphoblast. After a number of clonal divisions, the cells differentiate into effector and memory cells.

Effector $CD4^+$ and $CD8^+$ T cells have several possible roles in the immune response. Effector cells may secrete cytokines, chemokines, and other soluble factors that direct cells to become activated, to suppress other cells, to travel within the body, and to participate in the immune response. Most effector cells have a very short life in the body. After clearance of the target antigen, most effectors die via activation-induced cell death (AICD). However, a small number of cells survive after termination of the immune response, differentiating to memory cells. Memory T cells have long lifespans in the body and are able to respond very rapidly to repeat challenge with the same antigen.

However, in addition to occurring in the secondary lymphoid tissues, differentiation toward effector and memory phenotypes can also occur in tertiary lymphoid tissues (6). Tertiary lymphoid tissue consists of unencapsulated accumulations of lymphoid cells in locations other than the classical lymphoid organs. Tertiary lymphoid tissue bears organizational resemblance to lymph nodes and is thought to arise out of chronic inflammation related to non-resolving infection, autoimmune disease, cancer, and transplant rejection. Expression of the CCR7 ligand, CCL21, is sufficient to recruit naïve T cells into tertiary sites in mice and could play a role in naïve T cell recruitment in some human autoimmune diseases such as rheumatoid arthritis and ulcerative colitis (7). Once recruited to the tertiary site, the naïve T cells are retained by interaction through ICAM-1 or VCAM-1 on follicular dendritic cells or local stromal cells (8) and can receive differentiation signals.

Tertiary lymphoid tissue may have several alternative functions in the body. One role tertiary lymphoid tissue may serve is to control inflammation in the body. In artery tertiary lymphoid tissue, naïve $CD4^+$ T cells can be induced to become Treg cells, which are protective in atherosclerosis (9). Alternatively, in systemic autoimmune diseases such as systemic lupus

erythematosus and rheumatoid arthritis, tertiary lymphoid tissue can generate autoreactive T cells, which are associated with more severe disease (10). Our understanding of the role of tertiary lymphoid tissue in the body in health and disease is clearly still evolving.

Naïve T cell differentiation. Naïve $CD4^+$ T cells require two distinct signals for differentiation to occur, a signal through the TCR from the binding of cognate antigen presented in MHC and a signal through a costimulatory receptor on an APC. The classic T cell second signal is through CD28, although other costimulatory receptors exist including ICAM-1 (11), CTLA-4 (12), CD5 (13), and CD27 (14). Our lab has shown stimulating naïve $CD4^+$ T cells through the TCR as well as CD28 in the absence of exogenous cytokines promotes differentiation to T helper 1 (Th1) and T helper 2 (Th2) phenotypes but not T regulatory (Treg) cell phenotype (15). Conversely, stimulation through the TCR as well as ICAM-1 promotes differentiation to Th1 and Treg cells in the absence of exogenous cytokines but not Th2 cells (16), while stimulation through the TCR + CTLA-4 promotes differentiation to Treg through a different pathway than used by ICAM-1 costimulation (12). If only signal one is received, the cell will enter an unresponsive state known as anergy and ultimately die by apoptosis.

T cell subsets. There are many possible outcomes of $CD4^+$ T cell differentiation (**Figure 1.1**), with new phenotypes still being discovered. T helper 1 cells secrete proinflammatory cytokines such as interferon-γ and interleukin-12, activating cytotoxic T cells and macrophages to respond to viruses and other intracellular pathogens, as well as expressing the transcription

Figure 1.1

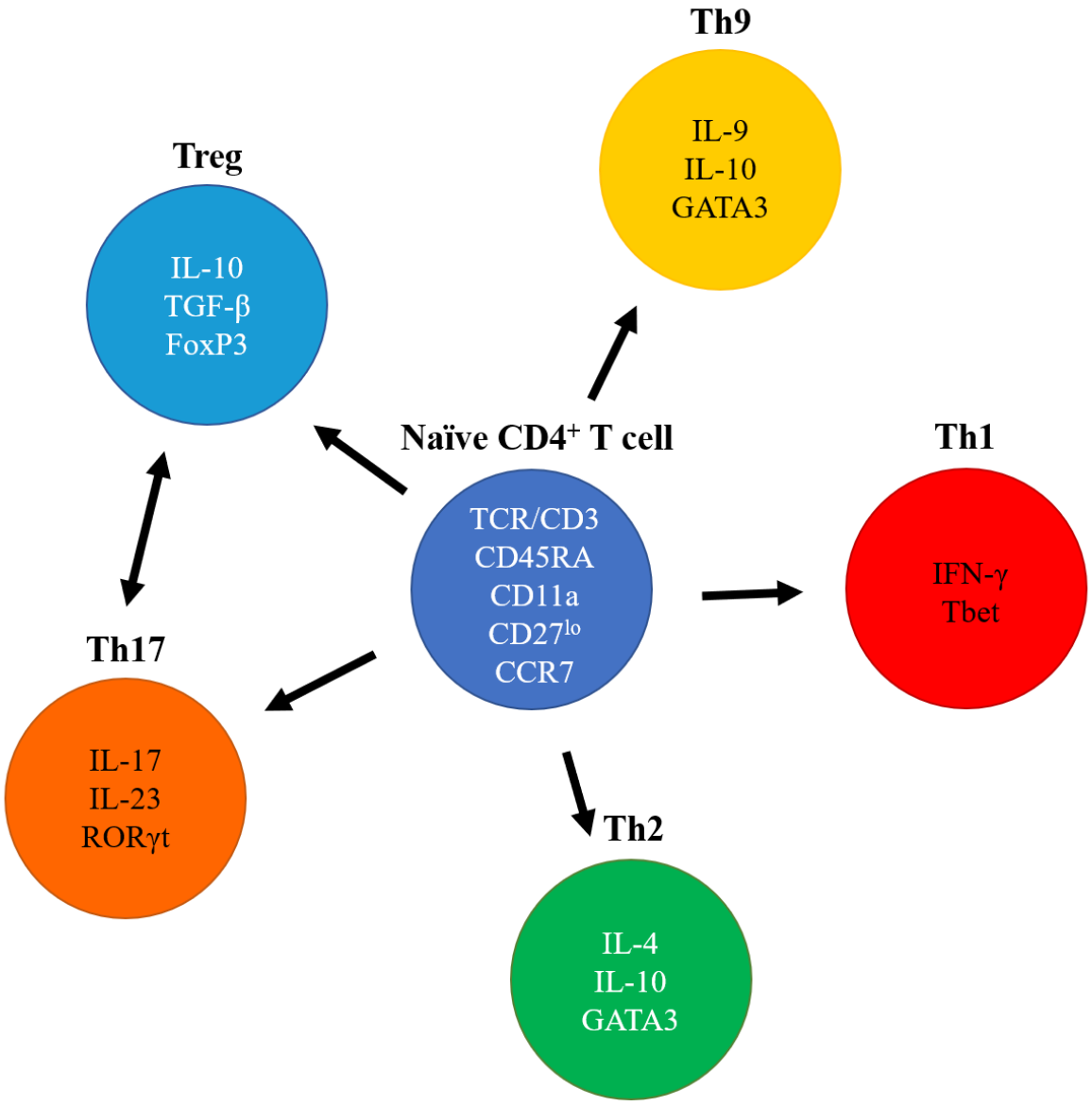

Figure 1.1 Diagram depicting some of the many potential phenotypic outcomes of naïve CD4$^+$ T cells. The naïve CD4$^+$ T cell (center, dark blue) may differentiate into a Th1 cell (right, red), Th2 cell (bottom, green), Th17 cell (lower left, orange), Treg cell (light blue, upper left), or a Th9 cell (upper right, yellow) depending on the specific costimulatory signals received by the naïve cell as well as the local cytokine environment.

factor T-bet. T helper 2 cells can be identified by expression of the transcription factor Gata3 and secrete interleukin-4 and interleukin-10, providing B cell help in situations of free-living bacteria, parasites, and playing a role in allergic reactions. T regulatory cells are characterized by expression of CD25, the high affinity IL-2 receptor (IL-2Rγ), as well as the other components of the IL-2 receptor and the transcription factor FoxP3, and they secrete interleukin-10 and TGF-β, which are generally suppressive cytokines.

The more recently discovered $CD4^+$ T cell phenotypes include T helper 17 cells and T helper 9 cells. T helper 17 cells are potent proinflammatory cells which secrete interleukin-17 and interleukin-23 and express the transcription factor RORγt. T helper 9 cells secrete interleukin-9, which stimulates cell proliferation in several hematopoietic cell types, as well as interleukin-10, and they express the transcription factor Gata3 (17).

ICAM-1. ICAM-1 (Intercellular adhesion molecule-1), also known as CD54, has five extracellular Ig domains which are glycosylated and contain disulfide bridges as well as a transmembrane domain followed by a short 28 amino acid cytoplasmic domain. The cytoplasmic domain has a single tyrosine residue which can be phosphorylated and is conserved among human, mouse, and rat (18). In addition, the cytoplasmic domain of ICAM-1 contains an SH3 binding domain and many positively-charged residues which could serve in recruiting and binding signal proteins (19). However, it is important to note that the SH3 binding domain is not conserved in murine or hamster ICAM-1 sequences (15), which could indicate that this domain is not functionally significant or that ICAM-1 functions differently among species.

The primary counter-receptor of interest of ICAM-1 with respect to T cell biology is integrin LFA-1 ($\alpha_L\beta_2$ or CD11a/CD18). LFA-1 on leukocytes binds to ICAM-1 on inflamed

tissue, playing a key role in the extravasation of immune cells. Additionally, ICAM-1 is used for attachment or entry by several pathogens, such as rhinovirus and *Plasmodium falciparum*-infected erythrocytes (20). ICAM-1 exists in native membrane-bound form as a non-covalent dimer, and dimerization correlates with dramatically enhanced binding of LFA-1 (18). ICAM-1 is widely expressed in the body, including endothelial cells, epithelial cells, fibroblasts, astrocytes, and leukocytes. On naïve and resting T lymphocytes, ICAM-1 is expressed at low levels but is upregulated on activation (21). Additionally, ICAM-1 can serve as a costimulatory molecule for T cells (11, 22).

The cytoplasmic domain of ICAM-1 is only 28 aa in human and lacks any catalytic activity. One study using rat T cells expressing truncated human ICAM-1 showed that the intracellular domain of ICAM-1 was essential for transendothelial migration, indicating a critical role for ICAM-1 signaling in T cells (16). Our lab has published the only extant data on the ICAM-1 signaling pathway in T cells in which we demonstrated that the cyclin dependent kinase cdc2 becomes transiently phosphorylated upon ICAM-1 crosslinking, and this phosphorylation correlates with inhibition of cdc2 activity in primary human T cells (23). However, studies in T cells as well as several other cell types suggest that ICAM-1 signals into the cell. Cortactin is time-dependently phosphorylated on tyrosine upon crosslinking of ICAM-1 in a rat endothelial cell line (24). Likewise, Lyn becomes phosphorylated on tyrosine in a mouse B cell lymphoma line when stimulated through ICAM-1 (25). p38 MAPK, ERK, and MKK3/6 are inducibly phosphorylated when stimulated through ICAM-1 in human airway epithelial cells (26). ICAM-1 associates with the actin cytoskeleton (27), most likely via interaction with ezrin (28-29).

CD28. CD28 is a membrane-bound, disulfide-linked glycosylated homodimer known as the prototypical T cell costimulatory receptor. CD28 is expressed on nearly all $CD4^+$ T cells and

most $CD8^+$ T cells (30). Unlike ICAM-1, CD28 has a single extracellular Ig variable-like domain. Its primary counter-receptors are B7-1 and B7-2, which are expressed on activated APCs. CD28 has a cytoplasmic YMNM consensus sequence which acts as a binding site for p85 of PI3K as well as Grb2 (31). CD28 also has a cytoplasmic PxxP motif which can be bound by SH3 domain-containing proteins (31).

This thesis. This thesis will investigate the potential effects on human health of the polycyclic aromatic hydrocarbons (PAHs) bisphenol A and pyrene on human naïve $CD4^+$ T cell differentiation, with emphasis on effector and memory cell differentiation, Th1/Th2/Treg differentiation, proliferation and cell death. Additionally, the thesis will compare two methods for naïve $CD4^+$ T cell isolation with respect to differentiation outcome and viability. Finally, I will briefly summarize my evaluation of peptides corresponding to the ICAM-1 binding domain for potential treatment of equine recurrent uveitis (ERU), identification of human T cell proteins which associate with ICAM-1, and identification of murine T cell proteins which associate with ICAM-1.

Chapter 1 references

1. Mark M. Davis and Yueh-Hsiu Chien, 2008. T cell antigen receptors. In *Fundamental Immunology*, 6th ed. W. E. Paul, ed. Wolters Kluwer Health: Lippincott Williams & Wilkins, Philadelphia, PA. p. 313-345.
2. S. C. De Rosa, L. A. Herzenberg, L. A. Herzenberg and M. Roederer, 2001, 11-color, 13-parameter flow cytometry: Identification of human naive T cells by phenotype, function, and T-cell receptor diversity. *Nat Med* 7: 245-248.
3. A. L. Dotson, 2012. Intercellular adhesion molecule-1 in T cell differentiation and as a target for peptide therapy of type 1 diabetes.
4. C. A. Dendrou, V. Plagnol, E. Fung, J. H. M. Yang, K. Downes, J. D. Cooper, S. Nutland, G. Coleman, M. Himsworth, M. Hardy, O. Burren, B. Healy, N. M. Walker, K. Koch, W. H. Ouwehand, J. R. Bradley, N. J. Wareham, J. A. Todd and L. S. Wicker, 2009, Cell-specific protein phenotypes for the autoimmune locus *IL2RA* using a genotype-selectable human bioresource. *Nat Genet* 41: 1011-1015.
5. M. L. Pekalski, R. C. Ferreira, R. M. R. Coulson, A. J. Cutler, H. Guo, D. J. Smyth, K. Downes, C. A. Dendrou, X. Castro Dopico, L. Esposito, G. Coleman, H. E. Stevens, S. Nutland, N. M. Walker, C. Guy, D. B. Dunger, C. Wallace, T. I. M. Tree, J. A. Todd and L. S. Wicker, 2013, Postthymic expansion in human CD4 naive T cells defined by expression of functional high-affinity IL-2 receptors. *J Immunol* 190: 2554-2566.
6. I. W. Nasr, M. Reel, M. H. Oberbarnscheidt, R. H. Mounzer, F. K. Baddoura, N. H. Ruddle and F. G. Lakkis, 2007, Tertiary lymphoid tissues generate effector and memory T cells that lead to allograft rejection. *Am J Transplan*t 7: 1071-1079.

7. W. Weninger, H. S. Carlsen, M. Goodarzi, F. Moazed, M. A. Crowley, E. S. Baekkevold, L. L. Cavanagh and U. H. von Andrian, 2003, Naive T cell recruitment to nonlymphoid tissues: A role for endothelium-expressed cc chemokine ligand 21 in autoimmune disease and lymphoid neogenesis. *J Immunol* 170: 4638-4648.
8. G. W. Jones, D. G. Hill and S. A. Jones, 2016, Understanding immune cells in tertiary lymphoid organ development: It is all starting to come together. *Frontiers in immunology* 7: 401-401.
9. D. Hu, Sarajo K. Mohanta, C. Yin, L. Peng, Z. Ma, P. Srikakulapu, G. Grassia, N. MacRitchie, G. Dever, P. Gordon, Francis L. Burton, A. Ialenti, Suleman R. Sabir, Iain B. McInnes, James M. Brewer, P. Garside, C. Weber, T. Lehmann, D. Teupser, L. Habenicht, M. Beer, R. Grabner, P. Maffia, F. Weih and Andreas J. R. Habenicht, 2015, Artery tertiary lymphoid organs control aorta immunity and protect against atherosclerosis via vascular smooth muscle cell lymphotoxin β receptors. *Immunity* 42: 1100-1115.
10. W. D. Shipman, D. C. Dasoveanu and T. T. Lu, 2017, Tertiary lymphoid organs in systemic autoimmune diseases: Pathogenic or protective? *F1000Research* 6: 196-196.
11. C. Chirathaworn, J. E. Kohlmeier, S. A. Tibbetts, L. M. Rumsey, M. A. Chan and S. H. Benedict, 2002, Stimulation through intercellular adhesion molecule-1 provides a second signal for T cell activation. *J Immunol* 168: 5530-5537.
12. A. N. Newton, 2014. Novel roles for CD23, CTLA-4 and lipoproteins in human T cell function and differentiation.
13. F. Spertini, W. Stohl, N. Ramesh, C. Moody and R. S. Geha, 1991, Induction of human T cell proliferation by a monoclonal antibody to CD5. *J Immunol* 146: 47-52.

14. K. A. Remedios, L. Meyer, B. Zirak, M. L. Pauli, H. A. Truong, D. Boda and M. D. Rosenblum, 2019, CD27 promotes CD4(+) effector T cell survival in response to tissue self-antigen. *J Immunol*

15. J. E. Kohlmeier, 2004. Intercellular adhesion molecule-1 (ICAM-1) influences T cell activation and development.

16. K. M. Williams, A. L. Dotson, A. R. Otto, J. E. Kohlmeier and S. H. Benedict, 2011, Choice of resident costimulatory molecule can influence cell fate in human naive CD4+ T cell differentiation. *Cell Immunol* 271: 418-427.

17. M. H. Kaplan, M. M. Hufford and M. R. Olson, 2015, The development and in vivo function of T helper 9 cells. *Nat Rev Immunol* 15: 295-307.

18. J. Greenwood, C. L. Amos, C. E. Walters, P.-O. Couraud, R. Lyck, B. Engelhardt and P. Adamson, 2003, Intracellular domain of brain endothelial intercellular adhesion molecule-1 is essential for T lymphocyte-mediated signaling and migration. *J Immunol* 171: 2099.

19. E. O. Long, 2011, ICAM-1: Getting a grip on leukocyte adhesion. *J Immunol* 186: 5021-5023.

20. P. L. Reilly, J. R. Woska, Jr., D. D. Jeanfavre, E. McNally, R. Rothlein and B. J. Bormann, 1995, The native structure of intercellular adhesion molecule-1 (ICAM-1) is a dimer. Correlation with binding to LFA-1. *J Immunol* 155: 529-532.

21. K. A. Roebuck and A. Finnegan, 1999, Regulation of intercellular adhesion molecule-1 (CD54) gene expression. *J Leukocyte Biol* 66: 876-888.

22. J. E. Kohlmeier, M. A. Chan and S. H. Benedict, 2006, Costimulation of naive human CD4+ T cells through intercellular adhesion molecule-1 promotes differentiation to a memory

phenotype that is not strictly the result of multiple rounds of cell division. *Immunology* 118: 549-558.

23. C. Chirathaworn, S. A. Tibbetts, M. A. Chan and S. H. Benedict, 1995, Cross-linking of ICAM-1 on T cells induces transient tyrosine phosphorylation and inactivation of cdc2 kinase. *J Immunol* 155: 5479-5482.
24. O. Durieu-Trautmann, N. Chaverot, S. Cazaubon, A. D. Strosberg and P. O. Couraud, 1994, Intercellular adhesion molecule 1 activation induces tyrosine phosphorylation of the cytoskeleton-associated protein cortactin in brain microvessel endothelial cells. *J Biol Chem* 269: 12536-12540.
25. J. Holland and T. Owens, 1997, Signaling through intercellular adhesion molecule 1 (ICAM-1) in a B cell lymphoma line. The activation of Lyn tyrosine kinase and the mitogen-activated protein kinase pathway. *J Biol Chem* 272: 9108-9112.
26. X. Wang, C. Lau, S. Wiehler, A. Pow, T. Mazzulli, C. Gutierrez, D. Proud and C. W. Chow, 2006, Syk is downstream of intercellular adhesion molecule-1 and mediates human rhinovirus activation of p38 MAPK in airway epithelial cells. *J Immunol* 177: 6859-6870.
27. O. Carpen, P. Pallai, D. E. Staunton and T. A. Springer, 1992, Association of intercellular adhesion molecule-1 (ICAM-1) with actin-containing cytoskeleton and alpha-actinin. *J Cell Biol* 118: 1223-1234.
28. L. Heiska, K. Alfthan, M. Gronholm, P. Vilja, A. Vaheri and O. Carpen, 1998, Association of ezrin with intercellular adhesion molecule-1 and -2 (ICAM-1 and ICAM-2). Regulation by phosphatidylinositol 4, 5-bisphosphate. *J Biol Chem* 273: 21893-21900.
29. H. M. Oh, S. Lee, B. R. Na, H. Wee, S. H. Kim, S. C. Choi, K. M. Lee and C. D. Jun, 2007, RKIKK motif in the intracellular domain is critical for spatial and dynamic organization of

ICAM-1: Functional implication for the leukocyte adhesion and transmigration. *Mol Biol Cell* 18: 2322-2335.

30. O. Acuto and F. Michel, 2003, CD28-mediated co-stimulation: A quantitative support for TCR signalling. *Nat Rev Immunol* 3: 939-951.
31. J. S. Boomer and J. M. Green, 2010, An enigmatic tail of CD28 signaling. *Cold Spring Harb Perspect Biol* 2: a002436.

Chapter 2. Polycyclic aromatic hydrocarbons (PAHs) influence human naïve $CD4^+$ T cell differentiation

Introduction

PAHs. Polycyclic aromatic hydrocarbons (PAHs) are compounds primarily produced during combustion of organic matter. Humans are exposed to PAHs in the form of car exhaust, cigarette smoke, plastics, grilled foods, and many others. PAH exposure has been linked to a wide variety of human diseases, including asthma, autoimmune diseases, leukemia, obesity, cardiovascular disease, and cancers (1-6). PAHs are hydrophobic and readily pass through cell membranes (7).

We chose to evaluate the effects of two specific PAH compounds on human T cell immunology. Those compounds are bisphenol A (BPA, alternatively known as 4,4'-isopropyllidenediphenol) and pyrene (benzo[*def*]phenanthrene).

BPA. BPA has two unconjugated phenolic rings (see **Figure 2.1**). Determining the effects of BPA on humans is of interest because BPA is becoming nearly ubiquitous in the environment, and its presence there is entirely due to anthropogenic activity, as BPA does not naturally occur. In fact, in 2007 the United States alone produced 5.3 billion kg of BPA, commercially valued at $2 billion (8). BPA is used as a raw material in the production of a wide variety of commercial products. 95% of all BPA produced is used to make polycarbonate plastic and epoxy resin. Products containing BPA include water bottles, coatings of food and beverage cans, CDs and DVDs, children's toys, food storage containers, tableware, medical devices, baby bottles, dental composites and sealants, even in antioxidants added to foods and cosmetics.

Figure 2.1

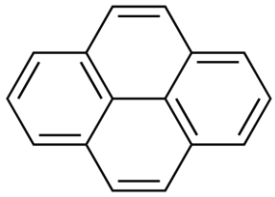

Figure 2.1 Chemical structure of the pyrene molecule.

Figure 2.2

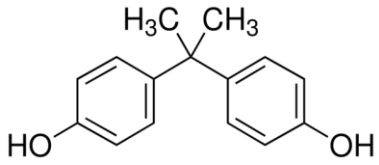

Figure 2.2 Chemical structure of the BPA molecule.

BPA is detectable at varying levels in air, water, and soil around the world, particularly near industrial manufacturing centers and landfills. However, the primary route of human exposure is dietary. It is thought that the principal sources of dietary BPA are canned foods lined with epoxy resins, drinking water in polycarbonate bottles, and saliva from individuals who have dental sealants and composites. BPA is metabolized in the liver or intestine and excreted through the kidneys with a half-life of 6 or more hours for orally ingested BPA (9-10). However, humans are continuously exposed to BPA, and BPA has been shown to partition to lipid-rich tissues, resulting in chronic exposure (11-13).

Data suggest BPA may affect humans by acting as an endocrine disruptor, a potential carcinogen, and a promoter of obesity and cardiovascular disease.

A large body of research supports the hypothesis that BPA can behave as an endocrine disruptor in humans. BPA is an agonist for human estrogen receptors as well as an antagonist for human androgen receptors (14), suggesting potential mechanisms for the observed endocrine disrupting effects of BPA. These effects include consistently higher rates of all types of sexual dysfunction in BPA-exposed male workers compared to unexposed workers (15). Further, BPA exposure is associated with earlier onset of puberty in males (16), and human testes treated with BPA ex vivo had significantly decreased testosterone production in a dose-dependent fashion (17).

BPA may also affect human reproduction. Serum BPA levels of the male partners of women undergoing in vitro fertilization are inversely correlated with embryo quality (18). Likewise, serum BPA levels in women undergoing in vitro fertilization inversely correlate with rate of fertilization; doubling of serum BPA level was associated with 55% decrease in the

probability of fertilization (19). One meta-analysis found that BPA directly negatively affects birthweight, preterm birth rates, developmental defects, and recurrent miscarriage in humans (20).

BPA exposure may also cause certain cancers. Early-life exposure to BPA seems to increase cancer risk in later life. For instance, fetal treatment of rats with BPA was associated with mammary carcinomas in up to 33% of adult rats (21). Another study found that fetal exposure to BPA was strongly associated with development of mammary carcinomas (22). These carcinomas were very large (>1 cm in diameter), and the serum levels of BPA in these rats was comparable to serum BPA levels observed in humans. Further, the association of BPA exposure with development of cancer is not limited to animal studies nor to mammary tissue cancers. One study of 60 urology patients showed a correlation between creatinine-adjusted urinary BPA levels and biopsy-confirmed prostate cancer, a link which was more pronounced in men younger than 65 years of age (23).

BPA exposure is further associated with obesity, both in humans as well as in rodent models. A large Canadian study of 4733 adults revealed a positive correlation with urinary BPA level and obesity defined by body mass index as well as increased waist circumference (24). Similarly, a meta-analysis of 61 rodent studies found significant positive associations between fetal BPA exposure and fat pad weight, triglyceride levels, and free fatty acids (25). Stronger positive associations were observed for male rodents as well as at BPA exposures below the US FDA reference dose of 50 μg/kg of body weight per day.

Data further suggest a relationship between BPA exposure and cardiovascular disease. In humans, both urinary (26) and serum (27) BPA levels are positively associated with

hypertension. Urinary BPA levels are also positively associated with cardiovascular diseases such as coronary heart disease, myocardial infarction, and angina (28-30).

Data on the effects of BPA in the immune system are somewhat variable. Prenatal BPA exposure may affect mice differently than adult exposure. BPA promotes T helper 1 immune and T helper 2 responses in prenatally exposed mice (31-32), while adulthood BPA exposure enhanced T helper 2 responses but not T helper 1, with a reduction in the percentage of $CD4^+$ $CD25^+$ cells (32). However, other groups found the BPA treatment of adult mice enhanced T helper 1 responses (33-35). Some studies found that BPA treatment increased splenocyte proliferation induced by the lymphocyte mitogen concanavalin A (35-36), while others report reduction in concanavalin A-induced splenocyte proliferation (33). One study in rats observed that perinatal BPA exposure was associated with severe colonic inflammation, a T helper 1 type response, which occurred in female rats only (37), while urinary BPA levels in humans correlate with childhood asthma, a T helper 2 dominated pathology (38). These disparate results suggest that further study on the influence of BPA on the immune system, particularly in humans is needed.

Pyrene. Pyrene is a peri-condensed PAH with four conjugated aromatic rings (see **Figure 2.2**). Pyrene is used in the manufacture of pesticides, dyes, and plastics, but it is also produced during incomplete combustion reactions such as the combustion of gasoline in an automobile engine, burning of wood and coal for heating and cooking, and burning of tobacco in cigarettes. Most human exposure to pyrene is via inhalation of air pollution in cities, including car exhaust, and wood, coal, or cigarette smoke, but occupational exposure and exposure through consumption of grilled or charred meat or other foods can also contribute.

Little is known concerning the effects of pyrene specifically on the human body, as the overwhelming majority of research conducted on pyrene-exposed cells or organisms employed a mixture of PAHs including pyrene rather than pyrene alone. Pyrene is thought to be involved in estrogen signaling, but its precise role is not clear (39). One study showed immunized mice treated with pyrene had enhanced antigen-induced IgE production, and splenic lymphocytes from the immunized mice had increased secretion of IL-4 when treated with pyrene in vitro (40). Both IgE and IL-4 are associated with a T helper 2 and allergic response. Similar results with respect to IgE production were obtained using pyrene-treated mice immunized with different allergens (41-43). Additionally, human peripheral blood mononuclear cells and peripheral T cells stimulated with concanavalin A exhibited dose-dependent increase in IL-4 protein and mRNA synthesis when treated with pyrene (43), further supporting the hypothesis that pyrene promotes a T helper 2/allergic type immune response. One additional study demonstrated that pyrene-treated primary human fibroblasts had enhanced production of IL-8 mRNA and protein (44). IL-8 is the chemokine CXCL8, which is known as an attractor and activator of neutrophils but may also play a role in airway inflammation because IL-8 can be produced by airway smooth muscle cells, among other cell types.

This chapter. Here we have isolated human $CD4^+$ naïve T cells from donated peripheral blood and treated them with BPA, pyrene, or DMSO during costimulation through CD28 or ICAM-1 to determine the effects of these compounds on differentiation outcome. We measured cell death, effector and memory differentiation, and T regulatory cell differentiation.

Materials and methods

Antibodies and reagents

Anti-CD3 (clone OKT3) was purchased from eBioscience (San Diego, CA), anti-CD28 (clone CD28.2) was purchased from BioLegend (San Diego, CA), and anti-ICAM-1 (clone R6.5) was purchased from BioXCell (West Lebanon, NH). Annexin V-PE, 7-Amino-Actinomycin D (7AAD), and anti-CD25-FITC (clone M-A251) were purchased from BD Pharmingen (San Jose, CA). Anti-CD11a-FITC (clone MEM-25) was purchased from Novus Biologicals (Littleton, CO), anti-CD27-PE (clone O323) was purchased from eBioscience (San Diego, CA), and anti-CD45RO-PerCP (clone UCHL1) was purchased from Invitrogen (Camarillo, CA). Anti-FoxP3-APC (clone 3G3) was purchased from Miltenyi Biotec (San Diego, CA). The isotype control was mouse IgG1-APC (eBioscience clone P3) for the FoxP3 antibody. The transcription factor staining buffer set for flow cytometry was purchased from eBioscience (San Diego, CA).

BPA (97% pure) was purchased from Sigma-Aldrich (St. Louis, MO) and aseptically dissolved in sterile DMSO (MP Biomedicals; Santa Ana, CA) at 0.3 mg/ml then diluted in DMSO to 3 μg/ml. 2 μL of 3 μg/ml BPA was added to the 200 μL total tissue culture well volume for final well concentration of 30 ng/ml BPA. Reagent-grade pyrene was purchased from Sigma-Aldrich (St. Louis, MO) and dissolved aseptically in sterile DMSO at 0.1 mg/ml, diluted in DMSO to 1 μg/ml, then 2 μl of 1 μg/ml pyrene was added to the tissue culture well of 200 μl total volume for a final concentration of 10 ng/ml pyrene. For the DMSO control, 2 μl neat sterile DMSO was added to each tissue culture well (total volume 200 μl).

Naïve T cells are primarily located in the blood and the lymphatics *in vivo,* so to determine how much BPA or pyrene to treat the naïve T cells with during the differentiation

experiments we examined the serum BPA and pyrene levels reported in the literature. The highest BPA levels are found in infants and children, but our blood donors were adults so we investigated published serum BPA levels from adults. BPA levels varied somewhat among individuals, investigations, men and women, and detection methods, ranging from below the limit of detection to 67.4 ng/ml (27, 45-49). However, the median serum level of BPA in adults in all studies here examined was approximately 1-3 ng/ml. Therefore, we chose to treat the naïve T cells with 30 ng/ml BPA for this project.

Serum measures of pyrene exposure in humans are very limited. No differences in serum pyrene levels has been observed between adults and children (unlike BPA), so we decided to include pyrene levels from children in our consideration. One study in adults found the mean level of pyrene in the serum to be 0.3 ng/ml (7) The only other serum pyrene level reported in the literature was a mean value of 1.1 ng/ml in sera from asthmatic children (50). Based on this information, we used 10 ng/ml as the experimental pyrene dose.

Cell purification

Heparinized peripheral whole blood (240 ml) was collected from healthy volunteer donors and diluted two parts blood into one part sterile TC-PBS (137 mM NaCl, 2.7 mM KCl, 1.5 mM KH_2PO_4, 9.6 mM Na_2HPO_4, 0.7 mM $CaCl_2$, 0.5 mM $MgCl_2$, and 10 mM glucose, pH 7.4) + 2% FBS + 1% penicillin/streptomycin. The PBMC layer was separated using Ficoll density gradient centrifugation, collected by pipette, washed in TC-PBS to remove residual Ficoll and platelets, and counted using a hemocytometer. The total yield of PBMC were further

purified to naïve $CD4^+$ T cells using the StemSep kit (cat#14155; StemCell, Vancouver, BC, Canada) according to the manufacturer. Purity was immediately assessed for each isolation by staining for CD11a, CD27, and CD45RO and analyzing by flow cytometry, gating on $CD11a^+$ $CD27^{lo}$ $CD45RO^{(-)}$ population.

Cell stimulation

Stimulating antibodies were diluted in sterile PBS to titrated lowest effective concentration. OKT3 (anti-CD3) was used at 1 μg/ml with either CD28.2 (anti-CD28) at 2 μg/ml or R6.5 (anti-ICAM-1) at 10 μg/ml. Antibody solutions were added to 96-well tissue culture-treated plates (TPP, Switzerland) and incubated for 2 hours at 37°C or overnight at 4°C. Wells were then washed 3X with sterile PBS to remove any unbound antibody. Cells were added to the wells at 1.5×10^6 cells/ml in RPMI 1640 (CellGro; Corning, New York) with 10% heat-inactivated fetal bovine serum (Atlanta Biologicals, Atlanta, GA), 50 IU/ml penicillin/50 μg/ml streptomycin (CellGro), and 2 mM L-glutamine (Gibco), and incubated at 37°C with 5% CO_2 for 7-14 days.

Flow cytometry

Cells were removed from the tissue culture plate by gentle pipetting. Cell proliferation was measured by CFSE dilution as we have previously described (51). Cells were labeled prior to stimulation using 2.5 μM 5-(and 6)-carboxyfluorescein diacetate succinimidyl ester (CFSE: Molecular Probes; Eugene, OR) from 5 mM stock solution in DMSO for 7 minutes at 37°C in

serum-free RPMI 1640. For cell death stain, cells were washed twice in cold PBS, stained in Annexin V binding buffer (0.01 M HEPES pH 7.4, 0.14 M NaCl, 2.5 mM $CaCl_2$) with Annexin V-PE (BD Pharnimgen, San Jose, CA) and 7AAD (7-aminoactinomycin D; BD Pharmingen), and washed once in Annexin V binding buffer prior to flow cytometry analysis. For all other stains, cells were blocked with 0.5% BSA in PBS for 15 minutes on ice, stained with fluorescent-tagged antibodies against cell surface targets for 1 hour in ice in the dark, washed once in cold PBS, and analyzed by flow cytometry. For evaluation of effector and memory differentiation, cells were stained with CD11a-FITC, CD27-PE, and CD45RO-PerCP. For transcription factor stains, cells were blocked and stained for surface targets first, then fixed, permeabilized, and stained for transcription factors using eBioscience transcription factor staining buffer kit. The Treg stain was anti-FoxP3-PE with anti-CD25-PECy5. Stained cells were then analyzed immediately using the Accuri C6 flow cytometer with CFlow software (Accuri Cytometers). Single color staining controls were used for compensation and isotype controls for gate placement.

Statistical analysis

GraphPad Prism software (GraphPad Software version 8.2.0, La Jolla, CA) was used to perform all statistical analysis. Statistical test used and significance level are indicated in figure legends.

Preliminary results

Due to unforeseen difficulties in cell purification (see Chapter 3) we were unable to obtain sufficient n values for some experiments. As such, these data are considered preliminary.

Treatment of human naïve CD4$^+$ T cells with BPA or pyrene during costimulation did not cause toxicity at Day 7.

The initial goal of this project was to establish whether BPA or pyrene would cause toxicity in naïve CD4$^+$ T cells at the experimental dosages during costimulation. Our lab routinely evaluates cell death by staining cells using fluorochrome-tagged Annexin V and 7-aminoactinomycin D (7AAD) as we have published previously (52). Annexin V is a protein that binds the cell membrane phospholipid phosphatidylserine. Phosphatidylserine is normally found only on the inner leaflet of the cell membrane but during the loss of membrane asymmetry that occurs during apoptosis, phosphatidylserine becomes exposed on the outer membrane leaflet. Using fluorochrome-labeled Annexin V, apoptosis can be sensitively detected in this way via flow cytometry. 7AAD is a fluorescent molecule which binds nucleic acids but does not pass through cell membranes. Dead and dying cells undergo loss of membrane integrity, causing their nucleic acids to be exposed and accessible by 7AAD. Cells which stain positively for both Annexin V and 7AAD are dead, while double negative cells are viable.

We investigated the number of dead cells using Annexin V/7AAD co-staining after treating naïve CD4$^+$ T cells with 30 ng/ml BPA, 10 ng/ml pyrene, or DMSO vehicle for 7 days during costimulation through ICAM-1 or CD28. **Figure 2.3** illustrates cell death during ICAM-1 costimulation for DMSO, BPA, or pyrene treated cells. The number of dead (Annexin V$^+$ 7AAD$^+$) BPA or pyrene treated cells was not significantly different from the number of dead

Figure 2.3

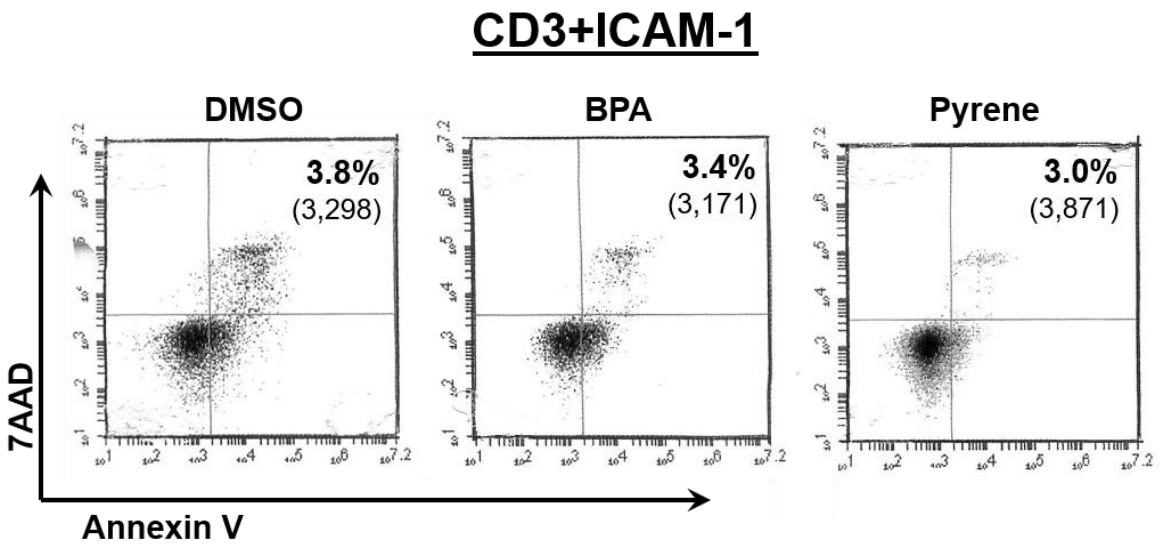

Figure 2.4

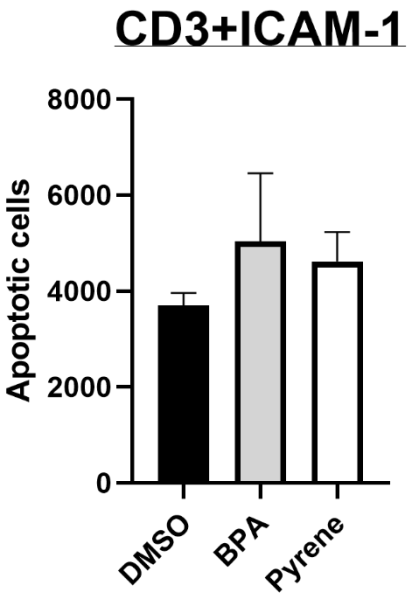

n=3

Figures 2.3-2.4. BPA and pyrene did not significantly affect apoptotic cell death during ICAM-1 costimulation of naïve CD4$^+$ T cells. Naïve CD4$^+$ T cells were stimulated through CD3+ICAM-1 in the presence of BPA, pyrene, or DMSO vehicle control for 7 days then stained with Annexin V and 7AAD and analyzed using flow cytometry. **2.3** Representative dot plots showing apoptosis stain with apoptotic cells in UR quadrant. Percent of apoptotic cells (Annexin V$^+$ 7AAD$^+$) given in bold, with number of apoptotic cells in parentheses. **2.4** Number of apoptotic cells after 7 days of costimulation with error bars indicating standard error, n=3.

Figure 2.5

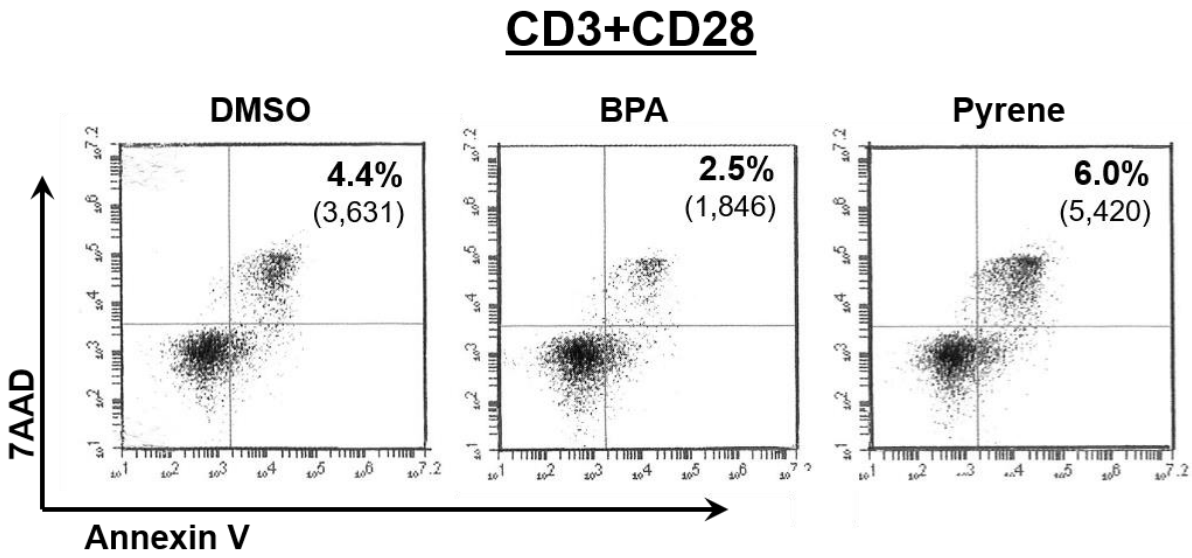

Figure 2.6

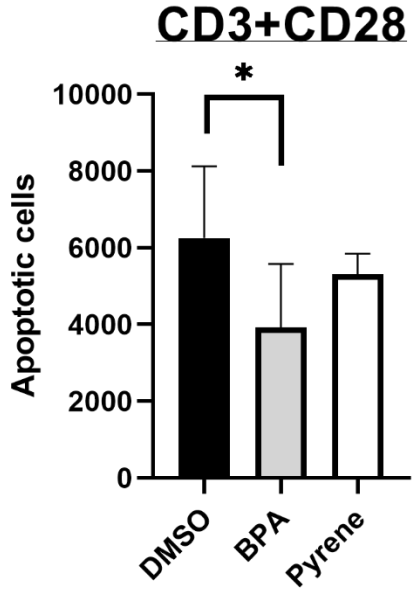

n=3

Figures 2.5-2.6. BPA was protective against cell death while pyrene did not significantly affect apoptotic cell death during CD28 costimulation of naïve CD4$^+$ T cells. Naïve CD4$^+$ T cells were stimulated through CD3+CD28 in the presence of BPA, pyrene, or DMSO vehicle control for 7 days then stained with Annexin V and 7AAD and analyzed using flow cytometry. **2.5** Representative dot plots showing apoptosis stain with apoptotic cells in UR quadrant. Percent of apoptotic cells (Annexin V$^+$ 7AAD$^+$) given in bold, with number of apoptotic cells in parentheses. **2.6** Number of apoptotic cells after 7 days of costimulation with error bars indicating standard error, n=3; *p<0.05 by paired two-tailed t test.

cells found in the DMSO vehicle control (**Figure 2.4**). For BPA, p=0.45 while for pyrene p=0.12 by paired two-tailed students t test.

Figure 2.5 depicts the number of dead cells during CD28 costimulation of DMSO, BPA, and pyrene treated naïve T cells. Treatment with BPA actually resulted in significantly fewer dead cells compared to the DMSO vehicle control (p<0.05 by paired two-tailed t test; **Figure 2.6**) while pyrene treatment did not significantly influence number of dead cells compared to DMSO control (p=0.61; **Figure 2.6**).

BPA and pyrene may promote proliferation of naïve CD4$^+$ T cells during CD28 and ICAM-1 costimulation.

Cell proliferation is an essential part of naïve T cell differentiation, and existing data on the effects of PAHs on proliferation is conflicting. As such, it was of interest to evaluate the influence of BPA and pyrene on naïve T cell proliferation.

Cell proliferation can be measured by staining the cells with the CFSE, which readily passes through the cell membrane and is crosslinked to intracellular proteins, becoming fluorescent when cleaved by the cell's esterases. Each time the cell divides, the dye is partitioned into the two daughter cells, becoming more dilute with each division. The fluorescence of the proliferating cells is then measured using a flow cytometer, with a fluorescence peak visible for each round of cell division in the resulting histogram.

Figure 2.7

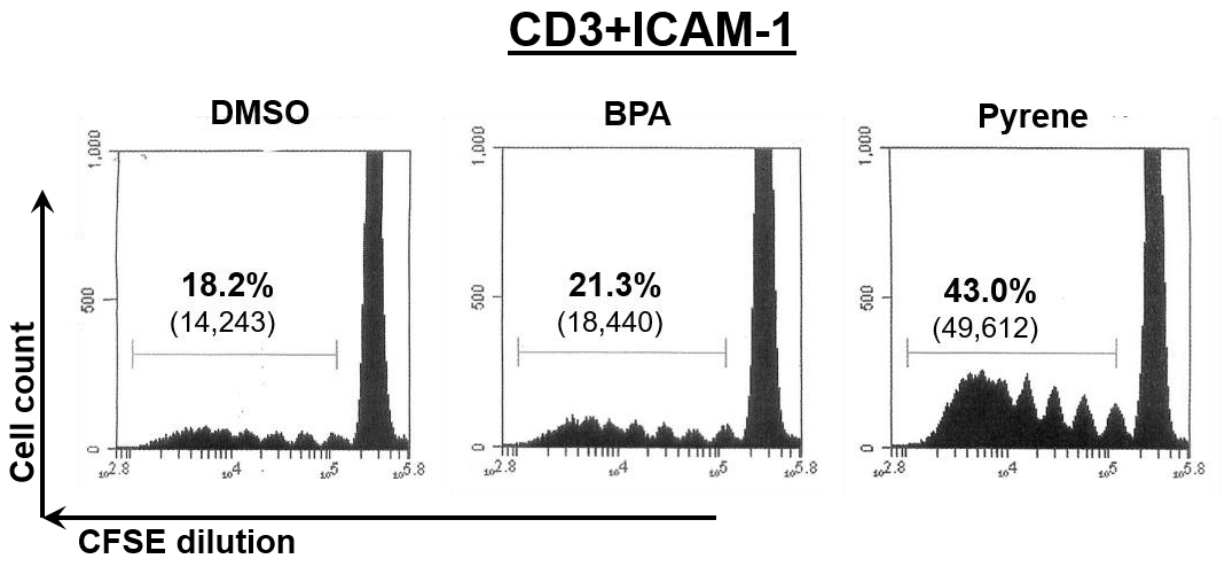

Figure 2.8

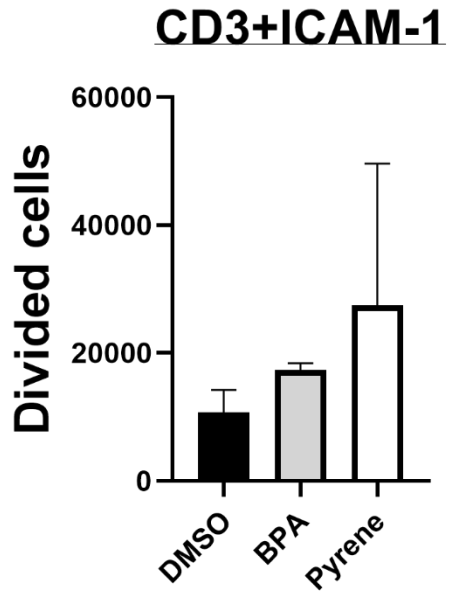

n=2

Figures 2.7-2.8. BPA or pyrene may promote cell proliferation during ICAM-1 costimulation of naïve CD4$^+$ T cells. Naïve CD4$^+$ T cells were stained with CFSE then stimulated through CD3+ICAM-1 in the presence of BPA, pyrene, or DMSO vehicle control for 7 days and analyzed using flow cytometry. **2.7** Representative CFSE histograms showing percentage of proliferated cells in bold above the gate; number of proliferated cells is given in parentheses. Representative of 2 experiments. **2.8** Number of proliferated cells after 7 days of costimulation with error bars indicating standard error, n=2.

Figure 2.9

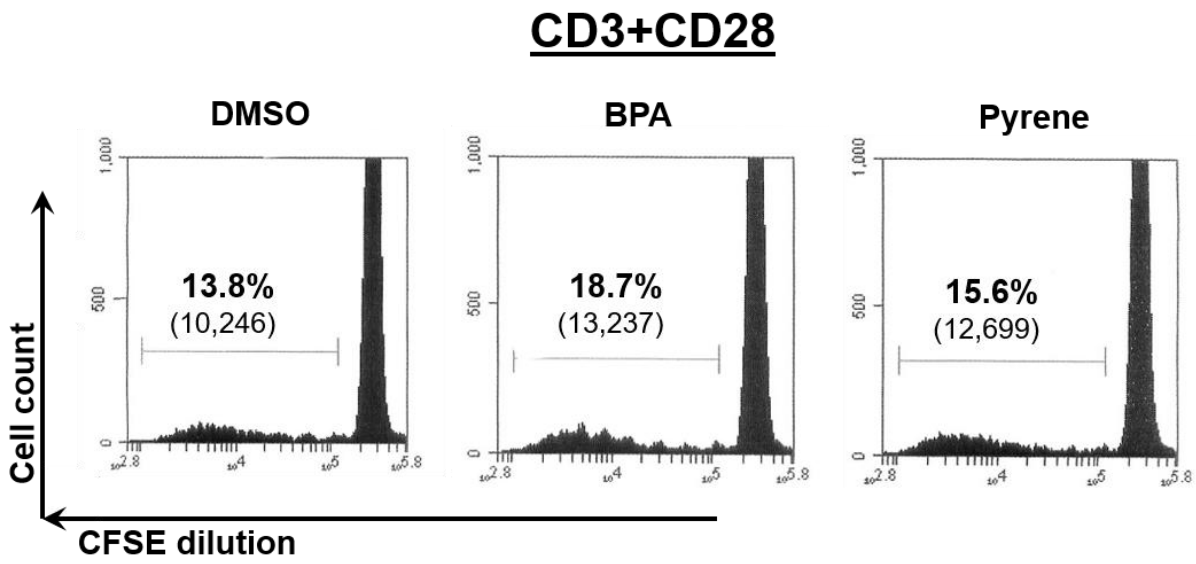

Figure 2.10

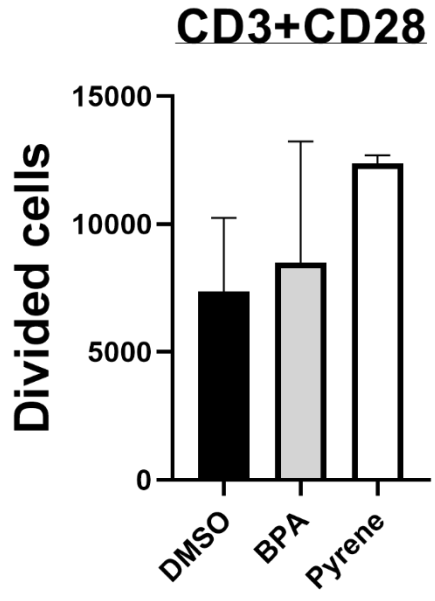

n=2

Figures 2.9-2.10. Exposure to pyrene during CD28 costimulation may promote cell proliferation. Naïve $CD4^+$ T cells were stained with CFSE then stimulated through CD3+CD28 in the presence of BPA, pyrene, or DMSO vehicle control for 7 days and analyzed using flow cytometry. **2.9** Representative CFSE histograms showing percentage of proliferated cells in bold above the gate; number of proliferated cells is given in parentheses. Representative of 2 experiments. **2.10** Number of proliferated cells after 7 days of costimulation with error bars indicating standard error, n=2.

Figure 2.7 shows representative CFSE histograms for naïve T cells treated with DMSO, BPA, or pyrene after 7 days of ICAM-1 costimulation. These preliminary data suggest a small increase in number of proliferated cells during BPA treatment compared to the DMSO vehicle control, with a more dramatic increase in proliferation resulting from pyrene treatment compared to DMSO control (**Figure 2.8**). However, it should be noted that n=2 for this experiment.

Number of proliferated naïve T cells during BPA, pyrene, and DMSO treatment after 7 days of CD28 costimulation is given in **Figure 2.9**. These preliminary data (n=2 due to loss of ability to isolate functional naïve T cells) suggest that BPA treatment did not affect the number of proliferated cells in CD28 costimulation and that pyrene may have increased the number of divided cells compared to the DMSO control (**Figure 2.10**).

Pyrene may reduce differentiation of effector and memory cells during ICAM-1 and CD28 costimulation of naïve T cells.

A critical step of elucidating any effects of BPA and pyrene exposure on naïve $CD4^+$ T cell differentiation and the overall immune response is measuring differentiation of the effector and memory cell populations during costimulation. To assess the effector and memory populations, we first gated on the CD45RO+ population, removing any remaining undifferentiated naïve cells from the analysis. Then we evaluated CD11a and CD27 expression. Naïve T cells start out in the upper left quadrant, $CD11a^{(-)}$ $CD27^+$. As they differentiate into effector cells, they migrate into the upper right quadrant, becoming $CD11a^+$ $CD27^+$. Finally, memory cells are found in the lower right quadrant, remaining $CD11a^+$ but becoming $CD27^{lo/(-)}$.

Figure 2.11

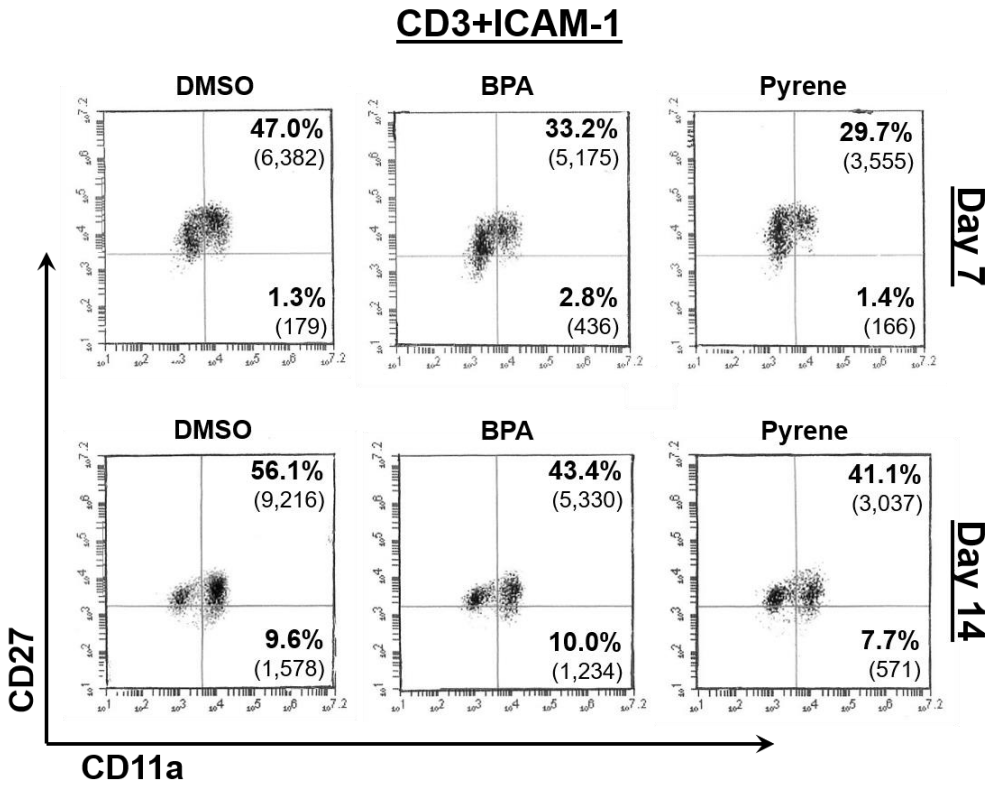

Figure 2.12

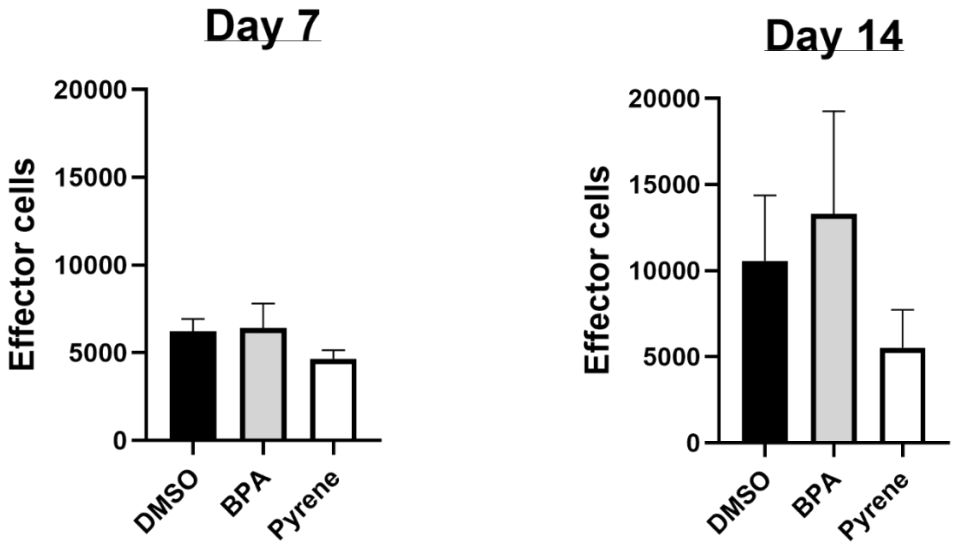

n=5-6

n=3-5

Figure 2.13

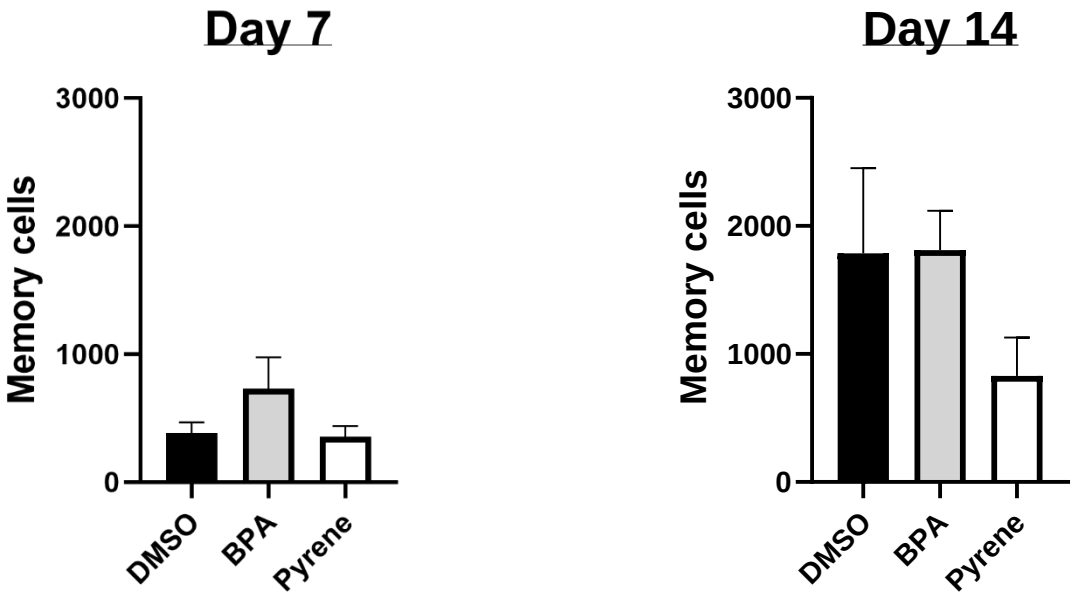

n=5-6 n=3-5

Figures 2.11-2.13. Exposure to pyrene during ICAM-1 costimulation may reduce effector and memory cell differentiation. Naïve $CD4^+$ T cells were stimulated through CD3+ICAM-1 in the presence of BPA, pyrene, or DMSO vehicle control and analyzed using flow cytometry at Day 7 and Day 14. **2.11** Representative flow cytometry dot plots gated on $CD45RO^+$ (differentiated) population showing percentage of effector cells ($CD45RO^+$ $CD11a^+$ $CD27^+$) in bold with number of effector cells in parentheses in the UR quadrant. Memory cells are shown in the LR quadrant ($CD45RO^+$ $CD11a^+$ $CD27^{(-)}$) with percentage of memory cells in bold and number of memory cells in parentheses. **2.12** Number of effector cells after 7 (left) or 14 (right) days of costimulation with error bars indicating standard error; n=5-6 (Day 7) or n=3-5 (Day 14). **2.13** Number of memory cells after 7 (left) or 14 (right) days of costimulation with error bars showing standard error; n=5-6 (Day 7) or n=3-5 (Day 14).

Figure 2.14

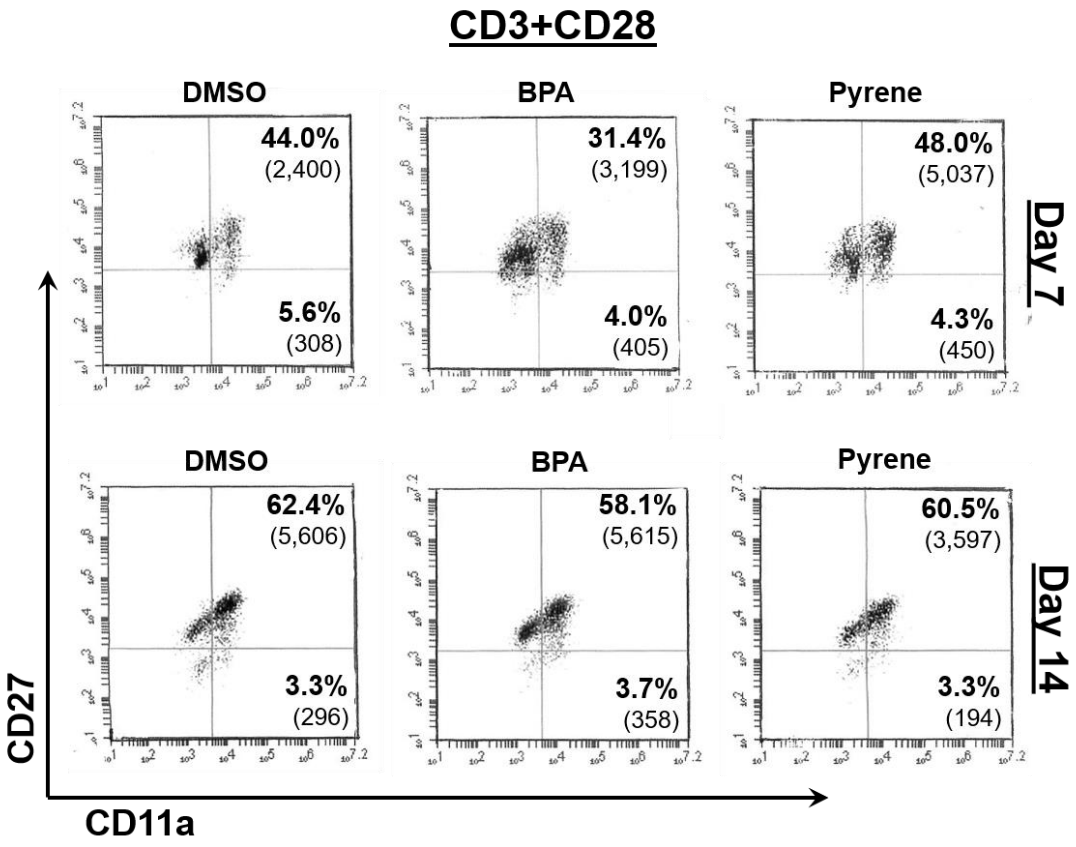

Figure 2.15

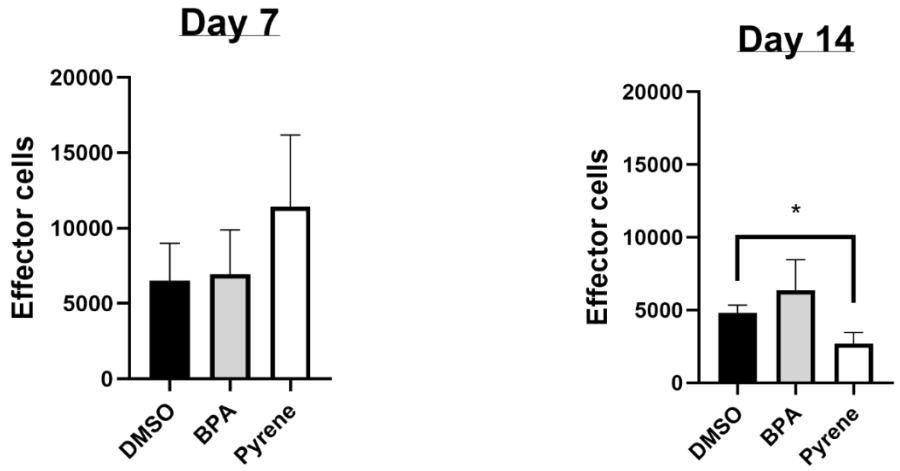

n=6-7

n=6

Figure 2.16

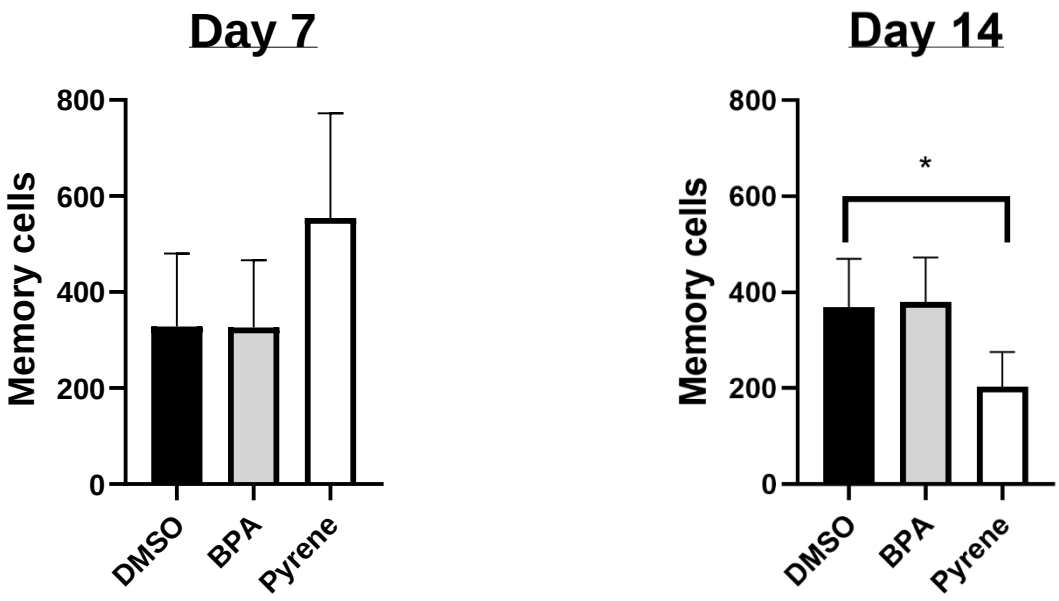

n=6-7 n=6

Figures 2.14-2.16. Exposure to pyrene during CD28 costimulation reduces effector and memory cell differentiation at Day 14. Naïve $CD4^+$ T cells were stimulated through CD3+CD28 in the presence of BPA, pyrene, or DMSO vehicle control and analyzed using flow cytometry at Day 7 and Day 14. **2.14** Representative flow cytometry dot plots gated on $CD45RO^+$ (differentiated) population showing percentage of effector cells ($CD45RO^+$ $CD11a^+$ $CD27^+$) in bold with number of effector cells in parentheses in the UR quadrant. Memory cells are shown in the LR quadrant ($CD45RO^+$ $CD11a^+$ $CD27^{(-)}$) with percentage of memory cells in bold and number of memory cells in parentheses. **2.15** Number of effector cells after 7 (left) or 14 (right) days of costimulation with error bars indicating standard error; n=6-7 (Day 7) or n=6 (Day 14). **2.16** Number of memory cells after 7 (left) or 14 (right) days of costimulation with error bars showing standard error; n=6-7 (Day 7) or n=6 (Day 14); *p<0.05 by paired t test.

We measured effector and memory cell differentiation during treatment with BPA, pyrene, or DMSO vehicle at 7 and 14 days of costimulation. **Figure 2.11** consists of representative dot plots gated on $CD45RO^+$ populations showing effector and memory populations of ICAM-1 costimulated naïve T cells at Day 7 (top row) and Day 14 (bottom row).

We observed that BPA and pyrene treatment had no impact on effector differentiation at Day 7 (**Figure 2.12**, left) but at Day 14, pyrene may have caused a non-significant reduction in effector cell numbers (**Figure 2.12**, right). Similarly, there was no effect on memory cell numbers (**Figure 2.13**) at Day 7 by either BPA or pyrene though at Day 14, the data suggest a non-significant reduction in memory cell number during ICAM-1 costimulation.

In **Figure 2.14**, we display CD11a versus CD27 dot plots gated on $CD45RO^+$ cell population of naïve T cells treated with BPA, pyrene, or DMSO during CD28 costimulation. BPA treatment did not influence number of effector cells at Day 7 or Day 14 (**Figure 2.15**). However, pyrene treatment may have non-significantly increased the number of effector cells at Day 7 though by Day 14 the number of effector cells was significantly lower for pyrene treatment compared to DMSO (**Figure 2.15**, $p<0.05$ by paired two-tailed t test). Likewise, BPA treatment did not alter the number of memory cells at Day 7 or Day 14 (**Figure 2.16**). Pyrene treatment may have non-significantly enhanced the number of memory cells present at Day 7; however the number of memory cells was significantly reduced for pyrene treatment at Day 14 compared to the DMSO control (**Figure 2.16**, $p<0.05$ by paired two-tailed t test).

Pyrene may inhibit differentiation of T regulatory cells during ICAM-1 costimulation.

Because we found that PAHs influenced effector and memory differentiation of naïve T cells, we wanted to evaluate the effects of these PAHs on differentiation of the $CD4^+$ T cell subsets. Differentiation of T regulatory cells is a major area of focus for our laboratory so naturally we investigated the effects of the PAHs on Treg differentiation. The standard method of evaluating T regulatory cell number is by staining the cells for the transcription factor FoxP3 and for CD25. T regulatory cells are $FoxP3^+$ $CD25^+$.

We measured differentiation of T regulatory cells from naïve $CD4^+$ T cells treated with BPA, pyrene, or DMSO after 10-12 days of ICAM-1 or CD28 costimulation. Representative dot plots with T regulatory cells in the upper right quadrant indicate number of T regulatory cells during ICAM-1 costimulation (**Figure 2.17**). We observed that BPA did not alter the number of T regulatory cells, but pyrene may have reduced the number of T regulatory cells differentiated (**Figure 2.18**). These preliminary data suggested that BPA and pyrene did not perturb T regulatory cell differentiation during CD28 costimulation (**Figures 2.19-20**).

Figure 2.17

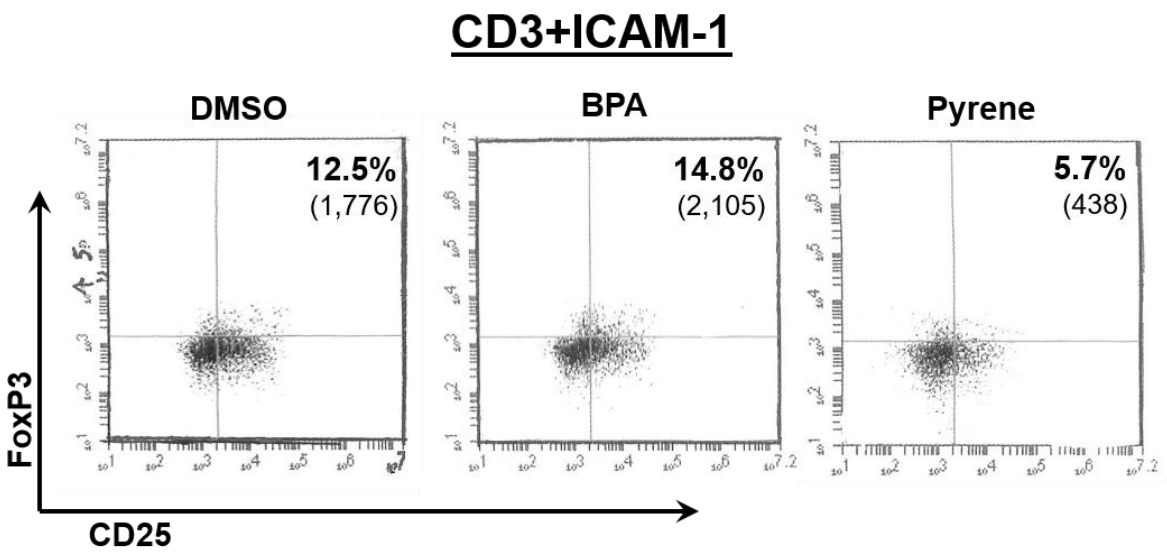

Figure 2.18

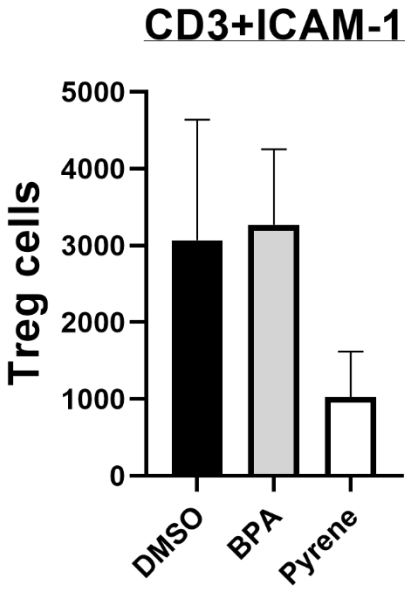

n=2-3

Figure 2.17-18. Exposure to pyrene during ICAM-1 costimulation may inhibit differentiation of Treg cells. Human naïve $CD4^+$ T cells were stimulated through CD3+ICAM-1 for 10-12 days in the presence of BPA, pyrene, or DMSO vehicle control then analyzed by flow cytometry for CD25 and FoxP3 expression. **2.17** Representative flow cytometry dot plots with Treg cells ($FoxP3^+$ $CD25^+$) shown in UR quadrant with percentage in bold and cell number in parentheses. **2.18** Graph shows mean number of Treg cells differentiated during ICAM-1 costimulation; error bars indicate SEM. Representative of 2-3 experiments.

Figure 2.19

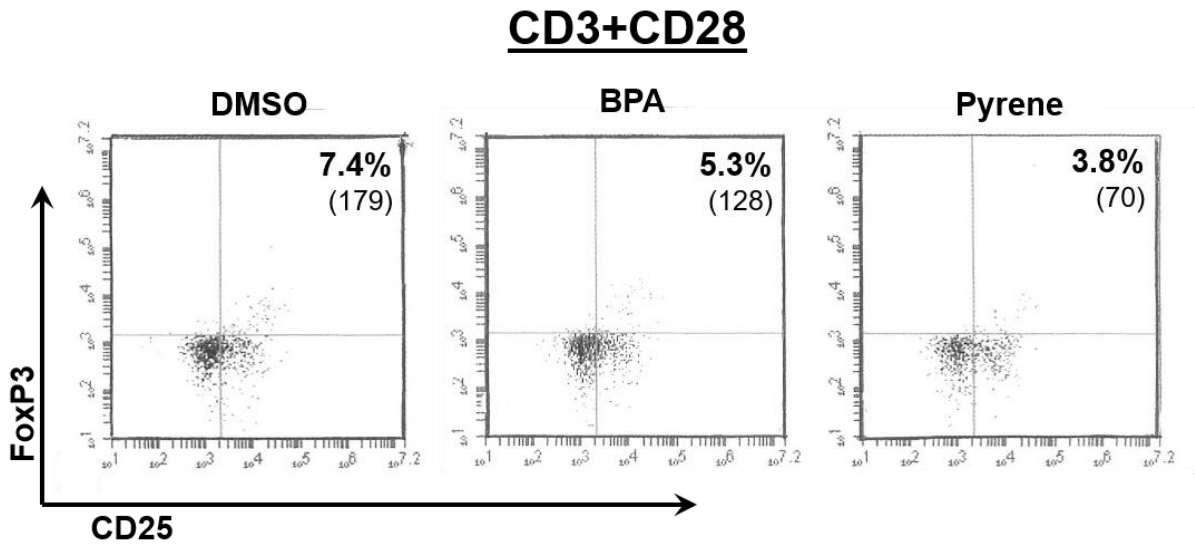

Figure 2.20

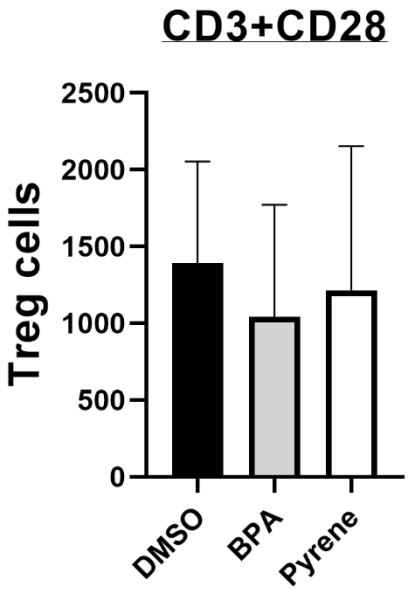

n=3

Figure 2.19-20. Treg differentiation during CD28 costimulation was not significantly affected by exposure to BPA or pyrene. Human naïve $CD4^+$ T cells were stimulated through CD3+CD28 for 10-12 days in the presence of BPA, pyrene, or DMSO vehicle control then analyzed by flow cytometry for CD25 and FoxP3 expression. **2.19** Representative flow cytometry dot plots with Treg cells ($FoxP3^+$ $CD25^+$) shown in UR quadrant with percentage in bold and cell number in parentheses. **2.20** Graph shows mean number of Treg cells differentiated during CD28 costimulation; error bars indicate SEM. Representative of 3 experiments.

Discussion

BPA and pyrene are ubiquitous in the human environment and exposure has been shown to have diverse consequences for human health, including the immune system. However, the effects of BPA and pyrene on human $CD4^+$ naïve T cell differentiation have yet to be determined. In the present work, we examined the effects of biologically relevant doses of BPA and pyrene on human naïve T cell proliferation and differentiation during costimulation.

We first verified that the experimental doses of BPA and pyrene were not toxic to naïve T cells during costimulation. We observed that 30 ng/ml BPA or 10 ng/ml pyrene did not affect cell death during ICAM-1 costimulation, but during CD28 costimulation, BPA reduced cell death while pyrene did not influence cell death. Therefore, we concluded that these levels of BPA and pyrene were not toxic to naïve T cells after 7 days of exposure.

Next, we investigated the effects of BPA and pyrene on naïve T cell proliferation as proliferation is a critical part of the naïve T cell differentiation process. Preliminary results suggested that BPA may have promoted a modest increase in proliferation during ICAM-1 costimulation but not CD28 costimulation, while pyrene may have promoted proliferation in both ICAM-1 and CD28 costimulations.

One method of evaluating effects on naïve T cell differentiation was to measure the effector and memory cell populations after 7-14 days of costimulation. We found that BPA treatment did not influence the number of effector or memory cells differentiated after 7 or 14 days of costimulation through ICAM-1 or CD28. However, pyrene treatment significantly reduced effector and memory cell numbers at Day 14 for CD28 costimulation only.

To further clarify the effects of BPA and pyrene on naïve T cell differentiation, we measured T regulatory cell differentiation in the presence of BPA or pyrene. Our preliminary results suggested that BPA did not affect Treg formation in ICAM-1 or CD28 costimulation but pyrene may have reduced Treg cell differentiation in the ICAM-1 costimulation only.

These data do not support a dramatic effect by BPA on human naïve T cell differentiation. There are many possible explanations for this result. One potential interpretation is that the DMSO control may also have been exposed to BPA through leaching from plastic pipet tips as well as the polystyrene tissue culture plate. Significant leaching of BPA from various plastics has been shown to occur at room temperature and 37°C (53). This leaching could have effectively caused all wells including the vehicle control to be exposed to enough BPA that we were unable to detect any effects of BPA treatment because the level of effective BPA exposure for the control and the BPA treatment were too similar.

Another possibility is that BPA has sex-specific effects. BPA is an estrogen agonist as well as an androgen antagonist (14), suggesting a potential avenue for sex-specific effects. Likewise, many studies in humans, mice, rats, and sheep have observed effects of BPA exposure which occurred only in females or only in males (4, 27, 37, 54-58). If any sex-specific BPA effects occurred in the present study, they may not be detectable here due to small experimental size.

The data for pyrene treatment suggested that pyrene may have promoted naïve T cell proliferation but inhibited differentiation to effector and memory cells and potentially also T regulatory cells. These observations do not easily reconcile with existing data on naïve T cell responses, though additional n values may clarify these observations. Further, while pyrene

inhibited effector and memory cell differentiation, it is unlikely to have induced anergy because the pyrene-treated cells had increased proliferation compared to the vehicle control, and anergic T cells do not proliferate or secrete IL-2, though they do express IL-2 receptors and respond to exogenous IL-2. Further studies involving measurement of IL-2 secretion, IL-2 receptor expression, and addition of IL-2 to pyrene-treated naïve T cells may help to illuminate the effects of pyrene with respect to anergy.

Another avenue of exploration would be to further characterize the population of proliferating but non-differentiating pyrene-treated naïve T cells. Of particular interest would be determining if pyrene-treated cells continue to express naïve T cell markers beyond CD45RO/CD11a/CD27, such as CD45RA, CCR7, and IL-7Rα. Should the pyrene-treated, costimulated T cells continue to express naïve markers, it may be interesting to assess the proliferative response of these cells to IL-7, a cytokine that is essential for naïve T cell homeostatic proliferation.

Here we have suggested that proliferation and differentiation of human naïve $CD4^+$ T cells was not strongly influenced by BPA treatment but pyrene may have enhanced proliferation while inhibiting effector and memory differentiation during costimulation. Further investigation would be required to determine how pyrene affects T cells and the immune response.

Chapter 2. References

1. A. N. Ananthakrishnan, E. L. McGinley, D. G. Binion and K. Saeian, 2011, Ambient air pollution correlates with hospitalizations for inflammatory bowel disease: An ecologic analysis. *Inflamm Bowel Dis* 17: 1138-1145.
2. N. C. Deziel, R. P. Rull, J. S. Colt, P. Reynolds, T. P. Whitehead, R. B. Gunier, S. R. Month, D. R. Taggart, P. Buffler, M. H. Ward and C. Metayer, 2014, Polycyclic aromatic hydrocarbons in residential dust and risk of childhood acute lymphoblastic leukemia. *Environ Res* 133: 388-395.
3. S. Ekblom-Kullberg, H. Kautiainen, P. Alha, M. Leirisalo-Repo and H. Julkunen, 2013, Smoking and the risk of systemic lupus erythematosus. *Clin Rheumatol*
4. D. K. Li, M. Miao, Z. Zhou, C. Wu, H. Shi, X. Liu, S. Wang and W. Yuan, 2013, Urine bisphenol-A level in relation to obesity and overweight in school-age children. *PLoS ONE* 8: e65399.
5. K. Nadeau, C. McDonald-Hyman, E. M. Noth, B. Pratt, S. K. Hammond, J. Balmes and I. Tager, 2010, Ambient air pollution impairs regulatory T-cell function in asthma. *J Allergy Clin Immunol* 126: 845-852 e810.
6. A. Alhamdow, C. Lindh, M. Albin, P. Gustavsson, H. Tinnerberg and K. Broberg, 2017, Early markers of cardiovascular disease are associated with occupational exposure to polycyclic aromatic hydrocarbons. *Scientific Reports* 7: 9426.
7. M. S. Neal, J. Zhu and W. G. Foster, 2008, Quantification of benzo[a]pyrene and other PAHs in the serum and follicular fluid of smokers versus non-smokers. *Reprod Toxicol* 25: 100-106.

8. Y. Q. Huang, C. K. C. Wong, J. S. Zheng, H. Bouwman, R. Barra, B. Wahlström, L. Neretin and M. H. Wong, 2012, Bisphenol A (BPA) in China: A review of sources, environmental levels, and potential human health impacts. *Environment International* 42: 91-99.
9. W. Volkel, T. Colnot, G. A. Csanady, J. G. Filser and W. Dekant, 2002, Metabolism and kinetics of bisphenol A in humans at low doses following oral administration. *Chem Res Toxicol* 15: 1281-1287.
10. R. W. Stahlhut, W. V. Welshons and S. H. Swan, 2009, Bisphenol A data in NHANES suggest longer than expected half-life, substantial nonfood exposure, or both. *Environ Health Perspect* 117: 784-789.
11. D. R. Doerge, N. C. Twaddle, M. Vanlandingham and J. W. Fisher, 2012, Pharmacokinetics of bisphenol A in serum and adipose tissue following intravenous administration to adult female CD-1 mice. *Toxicol Lett* 211: 114-119.
12. C. Han and Y. C. Hong, 2016, Bisphenol A, hypertension, and cardiovascular diseases: Epidemiological, laboratory, and clinical trial evidence. *Curr Hypertens Rep* 18: 11.
13. D. Melzer, N. E. Rice, C. Lewis, W. E. Henley and T. S. Galloway, 2010, Association of urinary bisphenol A concentration with heart disease: Evidence from NHANES 2003/06. *PLoS ONE* 5: e8673.
14. E. C. Bonefeld-Jorgensen, M. Long, M. V. Hofmeister and A. M. Vinggaard, 2007, Endocrine-disrupting potential of bisphenol A, bisphenol A dimethacrylate, 4-n-nonylphenol, and 4-n-octylphenol *in vitro*: New data and a brief review. *Environ Health Perspect* 115 Suppl 1: 69-76.

15. D. Li, Z. Zhou, D. Qing, Y. He, T. Wu, M. Miao, J. Wang, X. Weng, J. R. Ferber, L. J. Herrinton, Q. Zhu, E. Gao, H. Checkoway and W. Yuan, 2010, Occupational exposure to bisphenol-A (BPA) and the risk of self-reported male sexual dysfunction. *Hum Reprod* 25: 519-527.
16. Z. Wang, D. Li, M. Miao, H. Liang, J. Chen, Z. Zhou, C. Wu and W. Yuan, 2017, Urine bisphenol A and pubertal development in boys. *Int J Hyg Environ Health* 220: 43-50.
17. C. Desdoits-Lethimonier, L. Lesne, P. Gaudriault, D. Zalko, J. P. Antignac, Y. Deceuninck, C. Platel, N. Dejucq-Rainsford, S. Mazaud-Guittot and B. Jegou, 2017, Parallel assessment of the effects of bisphenol A and several of its analogs on the adult human testis. *Hum Reprod* 32: 1465-1473.
18. M. S. Bloom, F. S. Vom Saal, D. Kim, J. A. Taylor, J. D. Lamb and V. Y. Fujimoto, 2011, Serum unconjugated bisphenol A concentrations in men may influence embryo quality indicators during *in vitro* fertilization. *Environ Toxicol Pharmacol* 32: 319-323.
19. V. Y. Fujimoto, D. Kim, F. S. vom Saal, J. D. Lamb, J. A. Taylor and M. S. Bloom, 2011, Serum unconjugated bisphenol A concentrations in women may adversely influence oocyte quality during in vitro fertilization. *Fertil Steril* 95: 1816-1819.
20. V. Pergialiotis, P. Kotrogianni, E. Christopoulos-Timogiannakis, D. Koutaki, G. Daskalakis and N. Papantoniou, 2018, Bisphenol A and adverse pregnancy outcomes: A systematic review of the literature. *J Matern Fetal Neonatal Med* 31: 3320-3327.
21. T. J. Murray, M. V. Maffini, A. A. Ucci, C. Sonnenschein and A. M. Soto, 2007, Induction of mammary gland ductal hyperplasias and carcinoma *in situ* following fetal bisphenol A exposure. *Reprod Toxicol* 23: 383-390.

22. N. Acevedo, B. Davis, C. M. Schaeberle, C. Sonnenschein and A. M. Soto, 2013, Perinatally administered bisphenol A as a potential mammary gland carcinogen in rats. *Environ Health Perspect* 121: 1040-1046.

23. P. Tarapore, J. Ying, B. Ouyang, B. Burke, B. Bracken and S. M. Ho, 2014, Exposure to bisphenol A correlates with early-onset prostate cancer and promotes centrosome amplification and anchorage-independent growth *in vitro*. *PLoS ONE* 9: e90332.

24. M. T. Do, V. C. Chang, M. A. Mendez and M. de Groh, 2017, Urinary bisphenol A and obesity in adults: Results from the Canadian health measures survey. *Health Promot Chronic Dis Prev Can* 37: 403-412.

25. P. N. H. Wassenaar, L. Trasande and J. Legler, 2017, Systematic review and meta-analysis of early-life exposure to bisphenol A and obesity-related outcomes in rodents. *Environ Health Perspect* 125: 106001.

26. A. Shankar and S. Teppala, 2012, Urinary bisphenol A and hypertension in a multiethnic sample of us adults. *J Environ Public Health* 2012: 481641.

27. W. Aekplakorn, L. O. Chailurkit and B. Ongphiphadhanakul, 2015, Association of serum bisphenol A with hypertension in Thai population. *Int J Hypertens* 2015: 594189.

28. I. A. Lang, T. S. Galloway, A. Scarlett, W. E. Henley, M. Depledge, R. B. Wallace and D. Melzer, 2008, Association of urinary bisphenol A concentration with medical disorders and laboratory abnormalities in adults. *JAMA* 300: 1303-1310.

29. A. Shankar, S. Teppala and C. Sabanayagam, 2012, Bisphenol A and peripheral arterial disease: Results from the NHANES. *Environ Health Perspect* 120: 1297-1300.

30. D. Melzer, P. Gates, N. J. Osborne, W. E. Henley, R. Cipelli, A. Young, C. Money, P. McCormack, P. Schofield, D. Mosedale, D. Grainger and T. S. Galloway, 2012, Urinary

bisphenol A concentration and angiography-defined coronary artery stenosis. *PLoS ONE* 7: e43378.

31. S. Yoshino, K. Yamaki, X. Li, T. Sai, R. Yanagisawa, H. Takano, S. Taneda, H. Hayashi and Y. Mori, 2004, Prenatal exposure to bisphenol A up-regulates immune responses, including T helper 1 and T helper 2 responses, in mice. *Immunology* 112: 489-495.
32. H. Yan, M. Takamoto and K. Sugane, 2008, Exposure to bisphenol A prenatally or in adulthood promotes T_H2 cytokine production associated with reduction of $CD4^+CD25^+$ regulatory T cells. *Environ Health Perspect* 116: 514-519.
33. M. Alizadeh, F. Ota, K. Hosoi, M. Kato, T. Sakai and M. A. Satter, 2006, Altered allergic cytokine and antibody response in mice treated with bisphenol A. *J Med Invest* 53: 70-80.
34. M. Goto, Y. Takano-Ishikawa, H. Ono, M. Yoshida, K. Yamaki and H. Shinmoto, 2007, Orally administered bisphenol A disturbed antigen specific immunoresponses in the naive condition. *Biosci Biotechnol Biochem* 71: 2136-2143.
35. J. Y. Youn, H. Y. Park, J. W. Lee, I. O. Jung, K. H. Choi, K. Kim and K. H. Cho, 2002, Evaluation of the immune response following exposure of mice to bisphenol A: Induction of Th1 cytokine and prolactin by BPA exposure in the mouse spleen cells. *Arch Pharm Res* 25: 946-953.
36. M. Goto, H. Ono, Y. Takano-Ishikawa, H. Shinmoto and M. Yoshida, 2004, Mac1 positive cells are required for enhancement of splenocytes proliferation caused by bisphenol A. *Biosci Biotechnol Biochem* 68: 263-265.
37. V. Braniste, A. Jouault, E. Gaultier, A. Polizzi, C. Buisson-Brenac, M. Leveque, P. G. Martin, V. Theodorou, J. Fioramonti and E. Houdeau, 2010, Impact of oral bisphenol A

at reference doses on intestinal barrier function and sex differences after perinatal exposure in rats. *Proc Natl Acad Sci U S A* 107: 448-453.

38. K. M. Donohue, R. L. Miller, M. S. Perzanowski, A. C. Just, L. A. Hoepner, S. Arunajadai, S. Canfield, D. Resnick, A. M. Calafat, F. P. Perera and R. M. Whyatt, 2013, Prenatal and postnatal bisphenol A exposure and asthma development among inner-city children. *J Allergy Clin Immunol* 131: 736-742.
39. Y. Zhang, S. Dong, H. Wang, S. Tao and R. Kiyama, 2016, Biological impact of environmental polycyclic aromatic hydrocarbons (ePAHs) as endocrine disruptors. *Environmental Pollution* 213: 809-824.
40. T. Suzuki, T. Kanoh, M. Ishimori, S. Ikeda and H. Ohkuni, 1996, Adjuvant activity of diesel exhaust particulates (DEP) in production of anti-IgE and anti-IgG1 antibodies to mite allergen in mice. *J Clin Lab Immunol* 48: 187-199.
41. T. Suzuki, T. Kanoh, M. Kanbayashi, Y. Todome and H. Ohkuni, 1993, The adjuvant activity of pyrene in diesel exhaust on IgE antibody production in mice. *Arerugi* 42: 963-968.
42. T. Kanoh, T. Suzuki, M. Ishimori, S. Ikeda, M. Ohasawa, H. Ohkuni and Y. Tunetoshi, 1996, Adjuvant activities of pyrene, anthracene, fluoranthene and benzo(a)pyrene in production of anti-IgE antibody to Japanese cedar pollen allergen in mice. *J Clin Lab Immunol* 48: 133-147.
43. H. Bommel, M. Li-Weber, E. Serfling and A. Duschl, 2000, The environmental pollutant pyrene induces the production of IL-4. *J Allergy Clin Immunol* 105: 796-802.

44. H. Bömmel, M. Haake, P. Luft, J. Horejs-Hoeck, H. Hein, J. Bartels, C. Schauer, U. Pöschl, M. Kracht and A. Duschl, 2003, The diesel exhaust component pyrene induces expression of IL-8 but not of eotaxin. *Int Immunopharmacol* 3: 1371-1379.

45. V. Y. Fujimoto, D. Kim, F. S. vom Saal, J. D. Lamb, J. A. Taylor and M. S. Bloom, 2011, Serum unconjugated bisphenol A concentrations in women may adversely influence oocyte quality during in vitro fertilization. *Fertil Steril* 95: 1816-1819.

46. G. Schonfelder, W. Wittfoht, H. Hopp, C. E. Talsness, M. Paul and I. Chahoud, 2002, Parent bisphenol A accumulation in the human maternal-fetal-placental unit. *Environ Health Perspect* 110: A703-707.

47. Y. Ikezuki, O. Tsutsumi, Y. Takai, Y. Kamei and Y. Taketani, 2002, Determination of bisphenol A concentrations in human biological fluids reveals significant early prenatal exposure. *Hum Reprod* 17: 2839-2841.

48. L. N. Vandenberg, R. Hauser, M. Marcus, N. Olea and W. V. Welshons, 2007, Human exposure to bisphenol A (BPA). *Reprod Toxicol* 24: 139-177.

49. Q. Zhou, M. Miao, M. Ran, L. Ding, L. Bai, T. Wu, W. Yuan, E. Gao, J. Wang, G. Li and D. K. Li, 2013, Serum bisphenol-A concentration and sex hormone levels in men. *Fertil Steril* 100: 478-482.

50. N. M. Al-Daghri, M. S. Alokail, S. H. Abd-Alrahman, H. M. Draz, S. M. Yakout and M. Clerici, 2013, Polycyclic aromatic hydrocarbon exposure and pediatric asthma in children: A case-control study. *Environ Health* 12: 1.

51. J. E. Kohlmeier, L. M. Rumsey, M. A. Chan and S. H. Benedict, 2003, The outcome of T-cell costimulation through intercellular adhesion molecule-1 differs from costimulation through leucocyte function-associated antigen-1. *Immunology* 108: 152-157.

52. A. H. Newton and S. H. Benedict, 2014, Low density lipoprotein promotes human naive T cell differentiation to Th1 cells. *Hum Immunol* 75: 621-628.

53. J. Sajiki and J. Yonekubo, 2003, Leaching of bisphenol A (BPA) to seawater from polycarbonate plastic and its degradation by reactive oxygen species. *Chemosphere* 51: 55-62.

54. A. Bansal, C. Rashid, F. Xin, C. Li, E. Polyak, A. Duemler, T. van der Meer, M. Stefaniak, S. Wajid, N. Doliba, M. S. Bartolomei and R. A. Simmons, 2017, Sex- and dose-specific effects of maternal bisphenol A exposure on pancreatic islets of first- and second-generation adult mice offspring. *Environ Health Perspect* 125: 097022.

55. Y. Pu, J. D. Gingrich, J. P. Steibel and A. Veiga-Lopez, 2017, Sex-specific modulation of fetal adipogenesis by gestational bisphenol A and bisphenol S exposure. *Endocrinology* 158: 3844-3858.

56. S. E. Arambula, D. Jima and H. B. Patisaul, 2018, Prenatal bisphenol A (BPA) exposure alters the transcriptome of the neonate rat amygdala in a sex-specific manner: A CLARITY-BPA consortium study. *Neurotoxicology* 65: 207-220.

57. X. Xu, F. Dong, Y. Yang, Y. Wang, R. Wang and X. Shen, 2015, Sex-specific effects of long-term exposure to bisphenol-A on anxiety- and depression-like behaviors in adult mice. *Chemosphere* 120: 258-266.

58. K. A. McCaffrey, B. Jones, N. Mabrey, B. Weiss, S. H. Swan and H. B. Patisaul, 2013, Sex specific impact of perinatal bisphenol A (BPA) exposure over a range of orally administered doses on rat hypothalamic sexual differentiation. *Neurotoxicology* 36: 55-62.

Chapter 3. Human naïve $CD4^+$ T cells isolated using EasySep do not stimulate comparably to those isolated using StemSep

Introduction

Prior to 2015, we routinely isolated human naïve $CD4^+$ T cells from peripheral blood using the StemSep immunomagnetic negative selection kit, at which point StemCell approached us and indicated they planned to discontinue the StemSep kit we were using in favor of their new EasySep kit.

StemSep. StemSep (StemCell, cat#14155) labels non-naïve, non-$CD4^+$ cells with tetrameric selection antibodies (see **Figure 3.1**). One antibody in each tetramer binds to a specific protein that is found only on non-naïve cells, (see **Table 3.1** for list of selection Abs) while the other antibody in the tetramer binds to dextran. The tetramer-labeled cells are then mixed with dextran-coated magnetic particles, and the anti-dextran antibody binds to the dextran coating the magnetic particles. Next, the cell-tetramer-particle complexes are applied to a column. The column consists of stacked mesh layers made of alternating nonmagnetic and magnetic stainless steel inside a syringe barrel, which is suspended in a magnetic field. The labeled cells are retained by the magnetic field in the column, while the untouched naïve $CD4^+$ T cells pass through the column and are collected for downstream experimental use.

EasySep. The newer kit, EasySep (StemCell cat#19155), similarly labels non-naïve, non-$CD4^+$ T cells using negative selection tetrameric antibody complexes in which one antibody targets a non-naïve cell for removal (see **Table 3.1** for list of selection Abs) and the other antibody in the tetramer binds to dextran. However, the specific selection antibodies included in

Figure 3.1

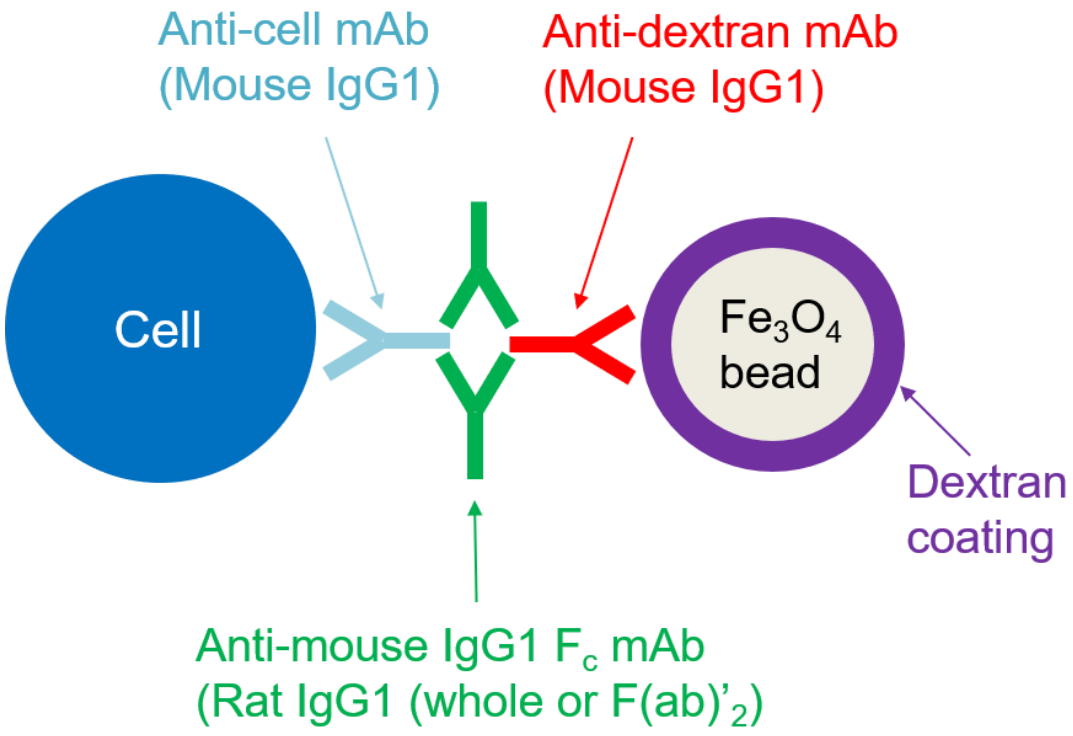
Anti-cell mAb
(Mouse IgG1)
Anti-dextran mAb
(Mouse IgG1)
Cell
Fe_3O_4
bead
Dextran
coating
Anti-mouse IgG1 F_c mAb
(Rat IgG1 (whole or $F(ab)'_2$)

Figure 3.1. Tetrameric antibody complex used in StemSep and EasySep isolations.

Antibody tetramers consisting of a mouse IgG1 anti-cell antibody (light blue) linked to an anti-dextran mouse IgG1 antibody (red) by two anti-mouse IgG1 Fc antibodies (green) are used to bind the target cell (dark blue) to the dextran-coated magnetic beads (purple), facilitating removal of the target cells by application of a strong magnetic field.

the cocktail differ considerably from those in the StemSep cocktail. Dextran-coated magnetic particles are added to the suspension and incubated to allow the anti-dextran antibodies to bind to the dextran-coated particles. The labeled cell suspension is placed in a strong magnetic field, and the labeled cells are retained in the magnetic field while the unlabeled, naïve cells are gently poured off. No column is employed in the EasySep isolation.

Magnetic particles. In addition to the divergent composition of the negative selection antibody cocktails in the StemSep and EasySep kits, the magnetic beads are also dissimilar. Both kits employ superparamagnetic iron oxide (Fe_3O_4) particles coated with dextran. However, the StemSep magnetic particles ("magnetic colloid") are 50-100 nm in diameter (1), and they are suspended in saline. The EasySep magnetic particles ("magnetic nanoparticles") are 150-450 nm in diameter (1) and are suspended in water. The increased size of the EasySep particles is necessitated by the column-free isolation method. There may be further proprietary differences between the two types of magnetic beads of which we are unaware. As such, it is possible that the differences between the StemSep and EasySep magnetic particles could contribute to our observed differences in the differentiation of StemSep and EasySep naïve T cells.

Antibody cocktails. Both StemSep and EasySep kits contain selection antibodies to CD45RO, CD8, CD14, CD16, CD19, CD56, and glycophorin A. However, EasySep has additional selection antibodies against CD20, CD25, CD36, CD61, CD66b, CD123, HLA-DR, and TCRγ/δ. Therefore, it is likely that one of more of the additional antibodies in the EasySep negative selection cocktail could contribute to the functional differences we have observed in the purified StemSep and EasySep naïve T cells.

Table 3.1

Ab target	Common name/cell target	StemSep	EasySep
CD45RO	Leukocyte common Ag (differentiated lymphocytes)	Y	Y
CD8	TCR (MHC I) co-receptor (cytotoxic Ts, NKs, DCs)	Y	Y
CD14	PAMP co-receptor for LPS (innate cells)	Y	Y
CD16	low affinity IgG FcR (NK cells, PMNs, MΦ)	Y	Y
CD19	B lymphocyte surface Ag B4 (BCR co-receptor, all B cells except plasma cells)	Y	Y
CD20	B lymphocyte Ag CD20 (all stages of B cell development except initial and final stages)		Y
CD25	IL-2Rα (activated lymphocytes)		Y
CD36	Platelet glycoprotein 4 (platelets, monocytes, RBCs)		Y
CD56	NCAM (NK cells)	Y	Y
CD61	β3 integrin (platelets)		Y
CD66b	CEACAM-8 (granulocytes)		Y
CD123	IL-3Rα (myeloid cells)		Y
TCR γ/δ	γ/δ T cells		Y
HLA-DR	MHC II (non-naïve)		Y
CD235	Glycophorin A (RBCs)	Y	Y

Table 3.1. Negative selection antibodies contained in StemCell's StemSep and EasySep human naïve $CD4^+$ T cell isolation kits indicated with "Y"s.

CD20. CD20 refers to the B lymphocyte antigen CD20 protein, which is primarily found on B cells at all stages of development except the initial and final stages. Inclusion of the CD20 antibody in the EasySep selection cocktail is most likely intended to further target B cells for removal, although the CD19 antibody found in both EasySep and StemSep is also intended to target B cells. However, CD20-expressing T cells have been detected in humans, both in a peripheral T cell lymphoma (2) as well as in healthy individuals, where $CD3^+$ $CD20^+$ T cells were found to make up 3-5% of the peripheral T cells in the blood (3). It is not known if there is a population of naïve T cells that expresses CD20.

CD25. The common name of CD25 is IL-2 receptor α-subunit. CD25 alone cannot transduce a signal into the cell upon ligand binding, but when complexed with IL-2Rβ and γ_c forms the high affinity IL-2 receptor. Among the pleiotropic effects of IL-2 signaling are T and B cell growth and expansion, induction of antibody production, and promotion of natural killer cell activity and activation-induced cell death. The ostensible purpose of anti-CD25 in the EasySep negative selection cocktail is to remove activated T cells, as CD25 is commonly said to be expressed on activated T cells. CD25 is also expressed on Tregs and on most resting $CD4^+$ memory cells. However, a study recently found a population of $CD4^+$ $CD45RA^+$ naïve T cells which express CD25 in the peripheral blood of adult humans (4). The size of the $CD25^+$ subset of naïve T cells increased with age, reaching approximately 20% of the naïve T cell population by age 40 (5). This suggests that the addition of the CD25 antibody to the EasySep selection cocktail could potentially remove a not-inconsiderable subset of naïve T cells from the population and thus alter the observed differentiation patterns from those of naïve cells purified using StemSep.

CD36. CD36 is a widely expressed membrane glycoprotein. In the blood, CD36 has been shown to be expressed on platelets, monocytes, macrophages, dendritic cells, and erythroid precursors. CD36 is a receptor for thrombospondin-1 in addition to being a scavenger receptor. CD36 binds lipids and lipoproteins from bacterial cell walls, fungal β-glucans, and *Plasmodium falciparum*-infected erythrocytes (6). Additionally, CD36 can recognize and internalize oxidized low-density lipoprotein, which in macrophages promotes the formation of proatherogenic foam cells (7-8). The CD36 antibody included in the EasySep negative selection cocktail is likely intended to target monocytes and macrophages as CD36 was originally identified as a monocyte/macrophage marker (9). Expression of CD36 on T cells, particularly naïve T cells, has not been determined.

CD61. CD61 is also known as β3 integrin, which is thought to be a marker for megakaryocytes and platelets. It is not known whether human T cells express CD61, but CD61 has been reported on the surface of canine peripheral blood lymphocytes (10). Since both EasySep and StemSep kits were designed for use with peripheral blood mononuclear cells (PBMCs) as the input, there should be few if any residual platelets in the starting cell population prior to StemSep or EasySep isolation. As such, inclusion of the CD61 antibody in the negative selection cocktail seems superfluous, assuming the intended target cell is indeed the platelet.

CD66b. CD66b is also referred to as CD67 and carcinoembryonic antigen related cell adhesion molecule 8 (CEACAM-8). CD66b is a member of the immunoglobulin super family. It is used to identify colorectal carcinomas but is also expressed in healthy tissues. CD66b is sometimes used as a marker of granulocyte activation, most frequently in neutrophils but it is also expressed on eosinophils (11). Again, because the starting cell population is PBMCs, there should be very few (if any) granulocytes present prior to the negative selection procedure.

Therefore, as with the CD61 antibody, the presence of anti-CD66b antibody in the selection cocktail for the purpose of removing granulocytes seems potentially gratuitous.

CD123. CD123 is the IL-3 receptor α-chain. CD123 must form a heterodimer with the cytokine common receptor β-chain to transduce signals. IL-3 produced by activated T cells as well as monocytes/macrophages, and it induces multipotent hematopoietic stem cells to differentiate into myeloid progenitors and activates basophils. CD123 is expressed on hematopoietic stem cells, basophils, acute myeloid leukemia cells, and T and B cell acute lymphoid leukemia cells (12). CD123 is also expressed on total $CD4^+$ T cells from healthy donors and is upregulated on these cells when costimulated through CD28 (13). It is not known whether human naïve T cells express CD123.

HLA-DR. HLA-DR (human leukocyte antigen-DR isotype) is an isotype of the major histocompatibility complex class II receptor, which presents short peptide antigens to the T cell receptor. HLA-DR is expressed on antigen presenting cells as well as peripheral T cells. Expression of HLA-DR has come into common use as a marker of T cell activation. However, one study found that only 23% of $HLA\text{-}DR^+$ $CD4^+$ T cells co-expressed CD25 (IL-2Rα), which is considered a classic T cell activation marker (14), suggesting that use of HLA-DR expression alone as an index of T cell activation may warrant reconsideration. The expression of HLA-DR in T cell subsets has not been established, including naïve T cells.

TCRγδ. TCRγδ refers to the T cell receptor composed of the γ and δ subunits. Most T cells in the blood express TCRαβ, which recognizes peptide antigens presented in MHC class II. However, a population of T cells express TCRγδ, which recognizes lipid antigens presented in CD1. The majority of T cells found in the skin are $TCR\gamma\delta^+$, but less than 5% of T cells in the

blood express γδ (15). As such, the number of γδ T cells in the PBMC population is expected to be very small, nevertheless the TCRγδ selection antibody is intended to target them for removal.

This chapter. This chapter will compare the naïve $CD4^+$ T cells isolated using StemSep and EasySep with respect to viability, proliferation, and differentiation. We will also attempt to identify components of EasySep that are responsible for the observed differences between the populations isolated by the two kits.

Materials and methods

Antibodies and reagents

Anti-CD3 (clone OKT3) was purchased from eBioscience (San Diego, CA), anti-CD28 (clone CD28.2) was purchased from BioLegend (San Diego, CA), and anti-ICAM-1 (clone R6.5) was purchased from BioXCell (West Lebanon, NH). Annexin V-PE and 7-Amino-Actinomycin D (7AAD) were purchased from BD Pharmingen (San Jose, CA). Anti-CD11a-FITC (clone MEM-25) was purchased from Novus Biologicals (Littleton, CO), anti-CD27-PE (clone O323) was purchased from eBioscience (San Diego, CA), and anti-CD45RO-PerCP (clone UCHL1) was purchased from Invitrogen (Camarillo, CA).

Cell purification

Heparinized peripheral whole blood (240 ml) was collected from healthy volunteer donors on three separate occasions at least 8 weeks apart and diluted two parts blood into one part sterile TC-PBS (137 mM NaCl, 2.7 mM KCl, 1.5 mM KH_2PO_4, 9.6 mM Na_2HPO_4, 0.7 mM $CaCl_2$, 0.5 mM $MgCl_2$, and 10 mM glucose, pH 7.4) + 2% FBS + 1% penicillin/streptomycin. The PBMC layer was separated using Ficoll density gradient centrifugation as we have previously reported (16-17), collected by pipette, washed in TC-PBS to remove residual Ficoll and platelets, and cells were counted using a hemocytometer. The PBMC from one blood draw per donor were further purified to naïve $CD4^+$ T cells using the StemSep kit (cat#14155; StemCell, Vancouver, BC, Canada) according to the manufacturer. The PBMC from the second blood draw from each donor was purified to naïve $CD4^+$ T cells using the EasySep kit (cat#19155; StemCell, Vancouver, BC, Canada) according to the manufacturer.

In attempt to identify problematic components of the EasySep kit, we divided PBMC from one donor into three equal aliquots. We isolated naïve $CD4^+$ T cells from one aliquot with the standard StemSep kit according to the manufacturer (StemSep selection cocktail and StemSep magnetic beads with column). The second aliquot was purified to $CD4^+$ naïve T cells using the StemSep selection cocktail and StemSep magnetic beads and column but with 100 µl CD25 antibody tetramer (from Human CD25 Positive Selection kit cat#18231; StemCell, Cambridge, MA) added to the StemSep selection cocktail per the $CD25^+$ deletion protocol in the CD25 Positive Selection kit tech sheet. The third aliquot was purified to naïve $CD4^+$ T cells using StemSep selection cocktail and EasySep beads (50 µl per EasySep tech sheet) and a column.

Purity was immediately assessed for each isolation by staining for CD11a, CD27, and CD45RO and analyzing by flow cytometry, gating on $CD11a^+$ $CD27^{lo}$ $CD45RO^{(-)}$ population.

Cell stimulation

Stimulating antibodies were diluted in sterile PBS to titrated lowest effective concentration. OKT3 (anti-CD3) was used at 1 µg/ml with either CD28.2 (anti-CD28) at 2 µg/ml or R6.5 (ICAM-1) at 10 µg/ml. Antibody solutions were added to 96-well tissue culture-treated plates (TPP, Switzerland) and incubated for 2 hours at 37°C or overnight at 4°C. Wells were then washed 3X with sterile PBS to remove any unbound antibody. Cells were added to the wells at 1.5×10^6 cells/ml in RPMI 1640 (CellGro, Corning, NY) supplemented with 10% heat-inactivated FBS (Atlanta Biologicals, Atlanta, GA) 50 IU/ml penicillin/50 µg/ml streptomycin (CellGro), and 2 mM L-glutamine (Gibco) and incubated at 37°C with 5% CO_2 for 7 days.

Flow cytometry

Cells were removed from the tissue culture plate by gentle pipetting. Cell proliferation was measured by CFSE dilution as previously described (16). Cells were labeled prior to stimulation using 2.5 μM 5-(and 6)-carboxyfluorescein diacetate succinimidyl ester (CFSE: Molecular Probes; Eugene, OR) from 5 mM stock solution in DMSO for 7 minutes at 37°C in serum-free RPMI 1640. For effector/memory stain, cells were blocked with 0.5% BSA in PBS, stained with CD11a-FITC, CD27-PE, and CD45RO-PerCP for 1 hour on ice in the dark, and washed once in cold PBS. For cell death stain, cells were washed twice in cold PBS, stained in Annexin V binding buffer (0.01 M HEPES pH 7.4, 0.14 M NaCl, 2.5 M $CaCl_2$) with Annexin V-PE and 7AAD, and washed once in Annexin V binding buffer. Stained cells were then analyzed using the Accuri C6 flow cytometer with CFlow software (Accuri Cytometers). Single color staining controls were used for compensation and gating.

Table 3.2

		PBMC	StemSep	EasySep	Percent yield
Donor A	#1	210	14.0		6.67
	#2	260	17.3		6.65
	#3	262		10.2	3.89
Donor B	#1	411	32.0		7.79
	#2	463	30.1		6.50
	#3	443		12.1	2.73

Table 3.2 EasySep isolation yields fewer human naïve $CD4^+$ T cells than StemSep isolation. 240 mL whole heparinized blood was collected from each volunteer donor on three separate occasions at least 8 weeks apart. PBMC were obtained from blood by Ficoll density gradient centrifugation and naïve $CD4^+$ T cells were isolated using either StemSep or EasySep negative selection kits. Yields are given in 10^6 cells and percent yield was calculated by dividing total number of naïve cells obtained by number of starting PBMC. Purity of the naïve cells was 98% or greater ($CD45RA^+RO^{(-)}$ $CD11a^{lo}$ $CD27^{(-)}$) for all isolations.

Preliminary results

The purified StemSep and EasySep naïve $CD4^+$ T cells appeared phenotypically similar by CD45RO/CD27/CD11a immediately after isolation. The purity by these three markers was comparable (~98% $CD45RO^{(-)}$ $CD27^+$ $CD11a^{(-)}$ for both StemSep and EasySep) though the yield of the EasySep naïve cells was somewhat lower than that of the StemSep naives when compared to the same blood donor (**Table 3.2**).

We also tested the StemSep and EasySep naïve T cells in our *in vitro* differentiation system. This system uses plate-bound antibodies to stimulate specific cell surface receptors mimicking cell-cell contact occurring during costimulation *in vivo*. We stimulated the cells through CD3+CD28, the T cell receptor and the classic T cell costimulatory receptor, as well as CD3+ICAM-1, the T cell receptor and an alternate costimulatory molecule, intercellular adhesion molecule-1. After 7 days of costimulation, we evaluated the results.

Costimulated EasySep naïve T cells do not appear to clump comparably to costimulated StemSep naïve T cells.

Microscopic observation of the T cells in the wells of the tissue culture plate after 7 days of costimulation rsuggested some differences among the cells isolated by the two methods. The CD3+ICAM-1 costimulated StemSep cells appeared densely distributed across the field with many large clumps present (**Figure 3.2**, top image). As we have previously published, clumping of T cells is an indication of activation (17). Similarly, many large cell clumps were present in CD3+CD28 stimulated StemSep T cells (**Figure 3.2**, center image). Conversely, no cell clumping was observed for CD3+ICAM-1 stimulated EasySep T cells, with cells appearing less

Figure 3.2

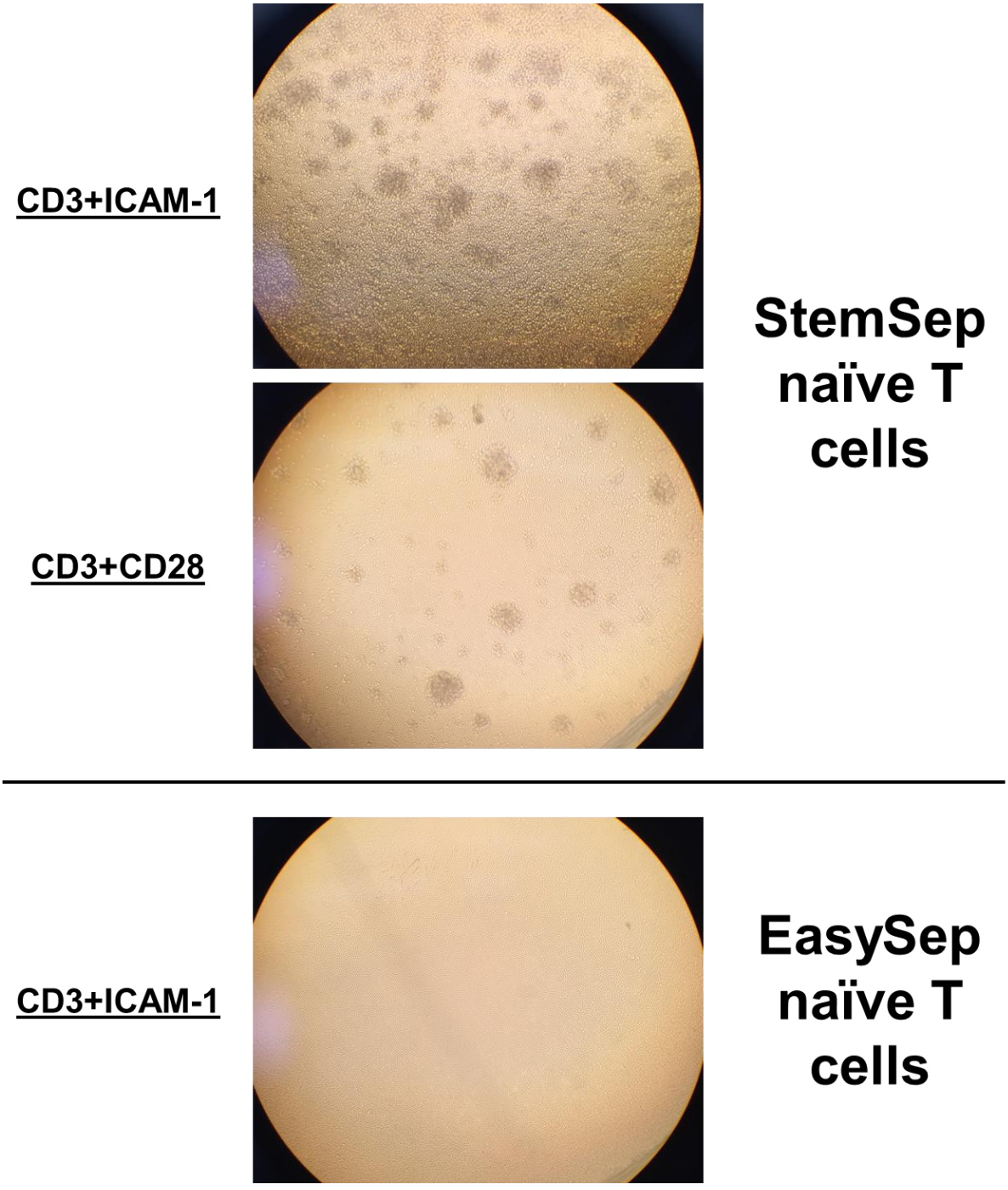
CD3+ICAM-1
CD3+CD28
StemSep naïve T cells
CD3+ICAM-1
EasySep naïve T cells

Figure 3.2 EasySep naïve T cells do not clump comparably to StemSep naïve T cells from the same donor during costimulation. Naïve $CD4^+$ T cells were purified from peripheral blood using either StemSep or EasySep and stimulated for 7 days through CD3+ICAM-1 or CD3+CD28 then photographed in situ at 100X magnification; n=1.

densely distributed in the well (**Figure 3.2**, bottom image). The CD3+CD28 stimulated EasySep cells resembled the CD3+ICAM-1 EasySep cells (data not shown).

EasySep naïve T cells had altered forward scatter versus side scatter flow cytometry profiles compared to StemSep naïve T cells after 7 days of costimulation.

We found that the StemSep naïve T cells differed from the EasySep naïve T cells after 7 days of costimulation by their flow cytometry forward scatter versus side scatter profiles (**Figure 3.3**). Forward scatter indicates the size of the particle moving past the detector while the side scatter shows granularity. The location of a particle in the forward scatter versus side scatter plot can be used to identify the type of particle. Intact, live T cells generally appear in the area enclosed by the green gates (**Figure 3.3**), while the activated and dividing blast cell population is shown in the blue gates and the dead and dying cell population is found in the red gates. The blue blast population was considerably reduced for both costimulations and both donors with EasySep compared to StemSep, and the red dead and dying cell population was likewise increased.

Cell death was dramatically increased for EasySep naïve T cells costimulated for 7 days compared to costimulated StemSep naïve T cells.

The amount of cell death of EasySep naïve T cells was different from that of StemSep naïve T cells after 7 days of costimulation. The percentage of dead (Annexin V^+ $7AAD^+$) cells in the ICAM-1 costimulations was 1.0-9.3% for StemSep naïve cells, while the percentage of dead EasySep naïve cells was 81.7-90.3% (**Figure 3.4**). Likewise, the percentage of dead CD28-

Figure 3.3

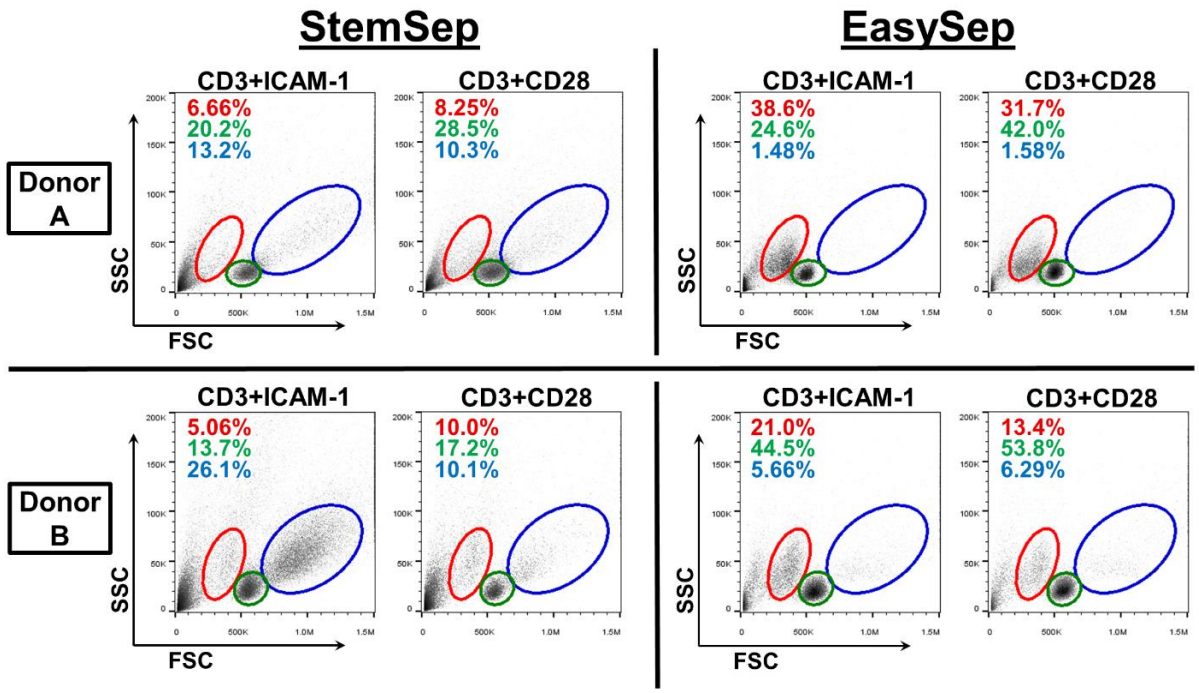
StemSep
EasySep
CD3+ICAM-1
CD3+CD28
Donor A
6.66%
20.2%
13.2%
8.25%
28.5%
10.3%
38.6%
24.6%
1.48%
31.7%
42.0%
1.58%
Donor B
5.06%
13.7%
26.1%
10.0%
17.2%
10.1%
21.0%
44.5%
5.66%
13.4%
53.8%
6.29%
SSC
FSC

Figure 3.3. Forward scatter versus side scatter profiles showed that EasySep naïve T cells had fewer blasts and more cell death compared to StemSep naïve T cells after 7 days of costimulation through ICAM-1 or CD28. Flow cytometry forward scatter (FSC) versus side scatter (SSC) plot comparing the StemSep naïve T cells (left) with the EasySep naïve T cells (right) of the same blood donor after 7 days of costimulation through CD3+ICAM-1 (left side plots) or CD3+CD28 (right side plots). The red gate and red percentage indicate the dead and dying cell population. The green gate and green percentage show the live cell population. The blue gate and blue percentage show the population of blasts; n=2.

Figure 3.4

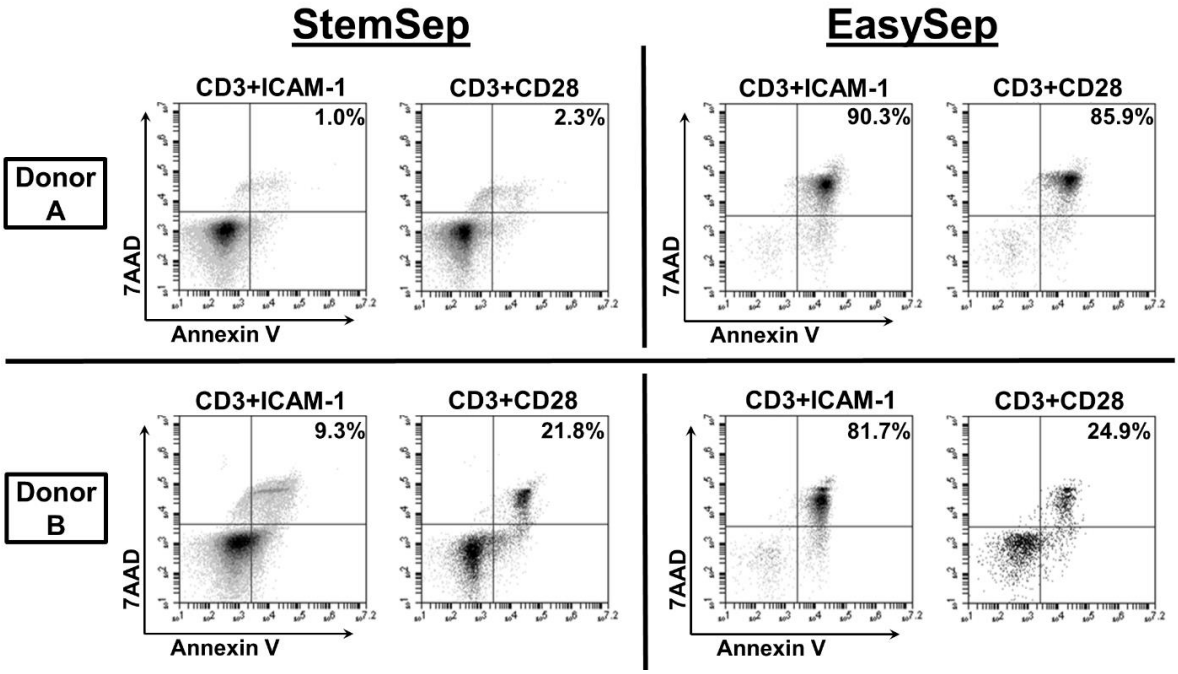
StemSep
EasySep
CD3+ICAM-1
CD3+CD28
CD3+ICAM-1
CD3+CD28
Donor A
1.0%
2.3%
90.3%
85.9%
7AAD
Annexin V
7AAD
Annexin V
CD3+ICAM-1
CD3+CD28
CD3+ICAM-1
CD3+CD28
Donor B
9.3%
21.8%
81.7%
24.9%
7AAD
Annexin V
7AAD
Annexin V

Figure 3.4 Cell death was dramatically increased in EasySep naïve T cells compared to StemSep naïve T cells from the same donor. Naïve T cells were purified from peripheral blood using either StemSep or EasySep and stimulated through CD3+ICAM-1 or CD3+CD28 for 7 days. Cells were then stained using Annexin V and 7AAD and analyzed by flow cytometry. Dead cells are Annexin V^+ $7AAD^+$ and located in the UR quadrant, with the percentage of dead cells given in bold for StemSep (left) and EasySep (right) naïve T cells; n=2.

costimulated StemSep naïve cells was 2.3-21.8% while the percentage of dead CD28-costimulated EasySep naïve T cells was 24.9-85.9% (**Figure 3.4**).

EasySep naïve T cells had dramatically reduced effector and memory cell differentiation compared to StemSep naïve T cells.

We compared the capacity of EasySep naïve T cells to differentiate into effector and memory cells with that of StemSep naïve T cells using flow cytometry. We gated on the $CD45RO^+$ (differentiated) cell population then assessed CD11a and CD27 expression to measure the effector and memory populations. For both donors and both ICAM-1 and CD28 costimulations, we observed a marked reduction in effector and memory cell populations in the EasySep naïve T cells. In the ICAM-1 costimulations, there were 33.5-45.5% effector and 5.4-18.6% memory for the StemSep naïve cells, while for the EasySep naïve cells there were 10.8-17.8% effector and 0-0.3% memory (**Figure 3.5A**). In the CD28 costimulations, there were 74.0-76.4% effectors and 8.3-12.8% memory for the StemSep naïve cells, and for the EasySep naïve cells there were 18.6-23.4% effectors and 2.5-3.3% memory (**Figure 3.5A**). Number of effector and memory cells is represented graphically in **Figure 3.5B**, with the bar indicating the mean. The cell numbers differed somewhat among the two donors as is commonly observed for primary human cells, but a strong visual trend in reduction of cell number for both EasySep effector and memory cells was apparent for both cell donors.

Figure 3.5

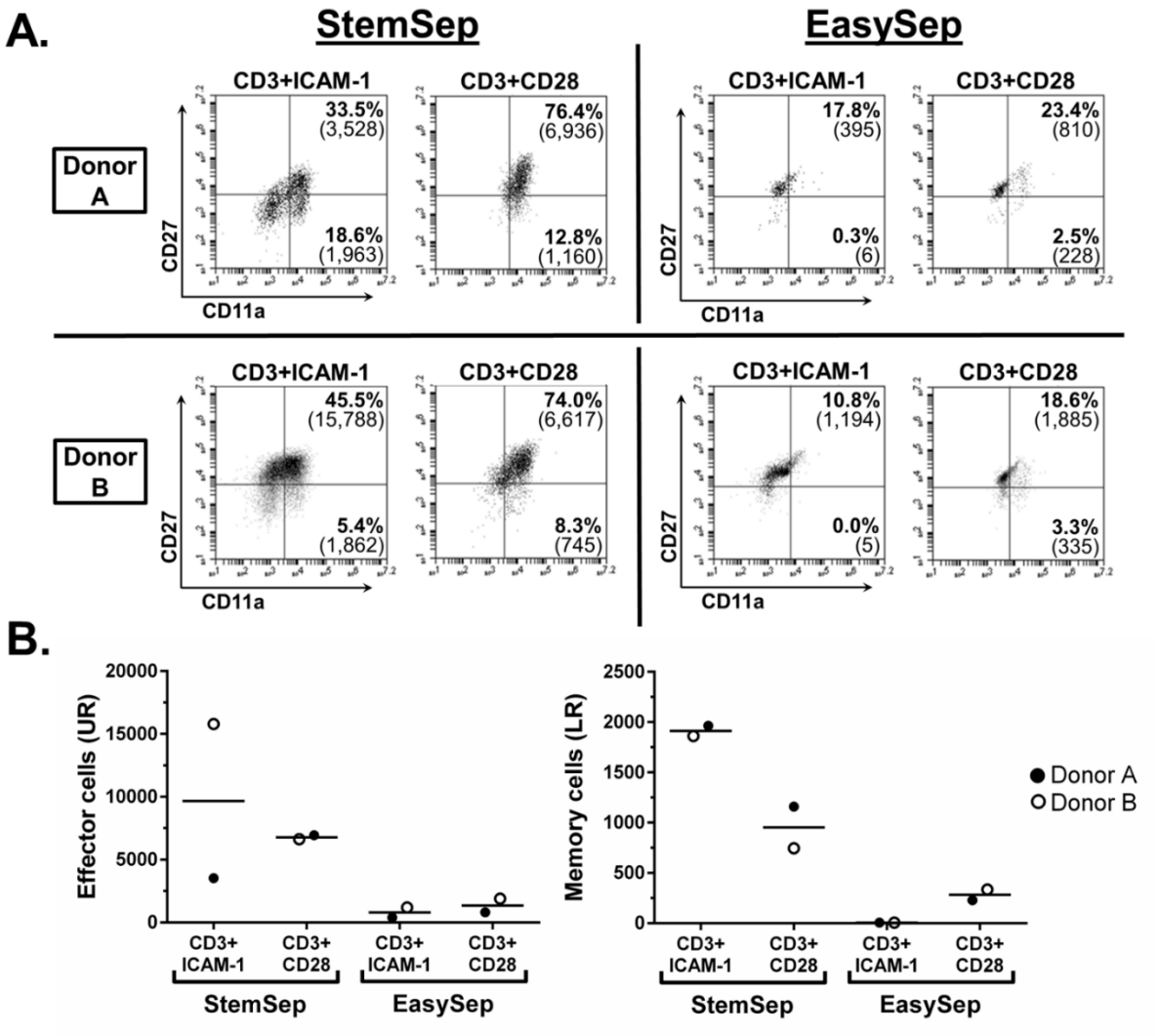
A.
StemSep
EasySep
CD3+ICAM-1
CD3+CD28
Donor A
33.5% (3,528)
18.6% (1,963)
76.4% (6,936)
12.8% (1,160)
17.8% (395)
0.3% (6)
23.4% (810)
2.5% (228)
Donor B
45.5% (15,788)
5.4% (1,862)
74.0% (6,617)
8.3% (745)
10.8% (1,194)
0.0% (5)
18.6% (1,885)
3.3% (335)
CD27
CD11a
B.
Effector cells (UR)
Memory cells (LR)
CD3+ ICAM-1
CD3+ CD28
StemSep
EasySep
Donor A
Donor B

Figure 3.5 EasySep naïve T cells showed markedly reduced effector and memory cell differentiation compared to StemSep naïve T cells from the same donor. Naïve T cells were purified from peripheral blood using either StemSep (left) or EasySep (right) and stimulated for 7 days through either CD3+ICAM-1 (left plot) or CD3+CD28 (right plot) then analyzed by flow cytometry. **A**. CD11a versus CD27 dot plots gated on $CD45RO^{+}$ population with effector cells in the UR quadrant and memory cells in the LR quadrant. Percentage of population is given in bold while cell number is in parentheses. **B**. Number of effector cells ($CD45RO^{+}$ $CD11a^{+}$ $CD27^{+}$) shown in the left-hand graph for StemSep and EasySep. Number of memory cells ($CD45RO^{+}$ $CD11a^{+}$ $CD27^{(-)}$) is shown in the right-hand graph for StemSep and EasySep. Bar indicates mean; n=2.

Inclusion of CD25 antibody in the selection cocktail and EasySep magnetic beads may both have reduced effector cell differentiation.

Having ascertained that naïve T cells isolated using EasySep have reduced effector and memory cell differentiation as well as increased cell death, we sought to identify which specific components of the EasySep kit were responsible for these results. Because the literature indicated that CD25 was indeed weakly expressed on naïve T cells (4-5), we hypothesized that removal of the $CD25^+$ population via the CD25 antibody tetramer included in the EasySep negative selection cocktail could potentially account for some of the observed differences among EasySep and StemSep naïve T cells. We therefore added CD25 antibody tetramer to the StemSep negative selection cocktail and used StemSep magnetic beads to isolate naïve T cells. We also wanted to verify that the EasySep beads themselves were not causing any of the observed differences among StemSep and EasySep naïve T cells, so we performed a naïve T cell isolation using StemSep negative selection cocktail with EasySep beads and a column to facilitate this comparison.

Preliminary results (n=1) suggested that addition of the CD25 tetramer reduced effector cell differentiation for ICAM-1 and CD28 costimulations, while the use of EasySep beads with the StemSep cocktail also resulted in reduced effectors (**Figure 3.6**). In the ICAM-1 costimulation (**Figure 3.6**, top row), there were 33,286 effector cells for the standard StemSep isolation, but there were only 12,273 effectors for StemSep+CD25 isolation and 1,679 effectors for the EasySep beads isolation. In the CD28 costimulation (**Figure 3.6**, bottom row), there were 30,857 effector cells for standard StemSep isolation, but for the StemSep+CD25 isolation there

Figure 3.6

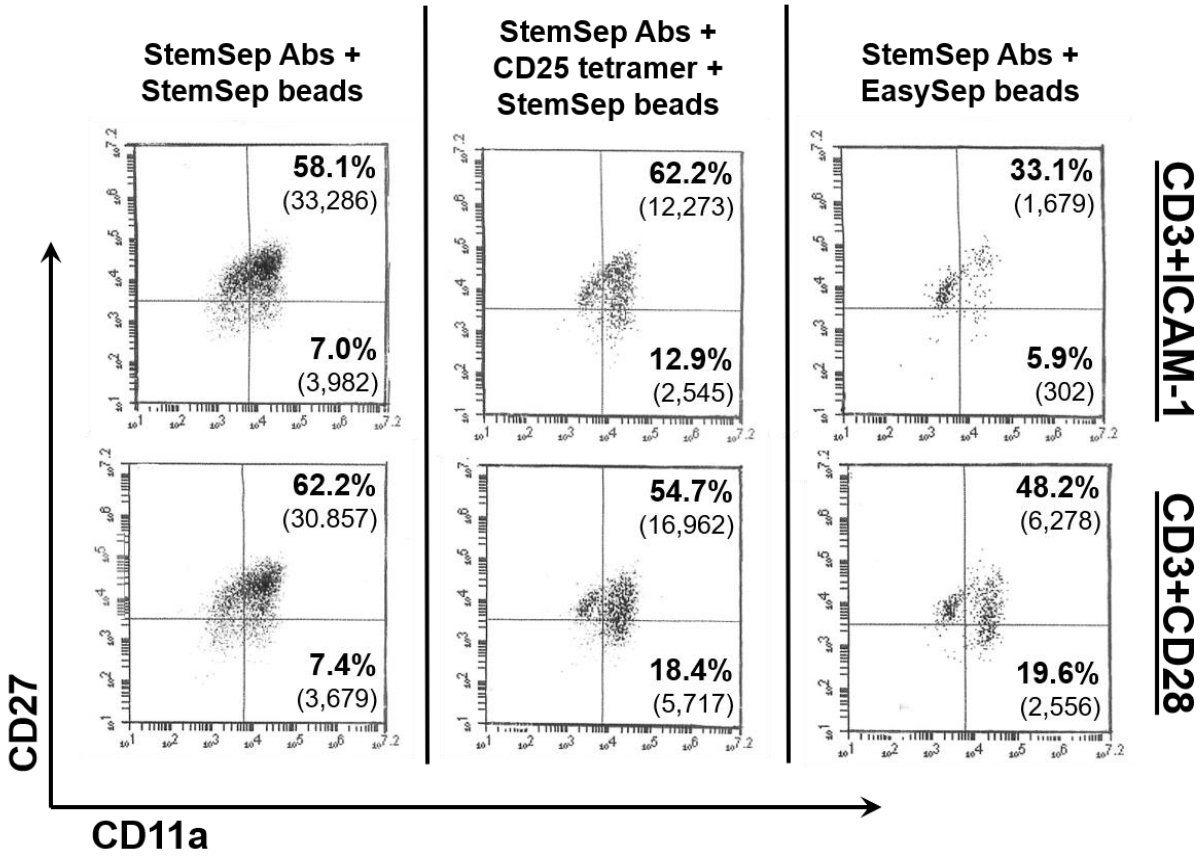
StemSep Abs + StemSep beads
StemSep Abs + CD25 tetramer + StemSep beads
StemSep Abs + EasySep beads
58.1% (33,286)
7.0% (3,982)
62.2% (12,273)
12.9% (2,545)
33.1% (1,679)
5.9% (302)
62.2% (30.857)
7.4% (3,679)
54.7% (16,962)
18.4% (5,717)
48.2% (6,278)
19.6% (2,556)
CD3+ICAM-1
CD3+CD28
CD27
CD11a

Figure 3.6 Addition of CD25 antibody tetramer to negative selection cocktail or use of EasySep beads reduced differentiation of effector cells. Naïve T cells were purified from peripheral blood using standard StemSep isolation (StemSep antibody cocktail with StemSep magnetic beads; left); StemSep isolation with the addition of CD25 antibody tetramer to the antibody cocktail and StemSep magnetic beads (center); or StemSep antibody cocktail with EasySep magnetic beads (right). Naïve T cells from each isolation were stimulated through CD3+ICAM-1 (top row) or CD3+CD28 (bottom row) for 7 days before analysis by flow cytometry. All plots are gated on the $CD45RO^+$ population with effector cells shown in the UR quadrant ($CD11a^+$ $CD27^+$) and memory cells in the LR quadrant ($CD11a^+$ $CD27^{lo/(-)}$). Percentage of cells in the quadrant is given in bold while cell number is in parentheses; n=1.

were 16,962 effectors and for the EasySep beads isolation there were 6,278 effectors. There were also fewer overall $CD45RO^+$ cells in the StemSep+CD25 and EasySep beads isolations.

Addition of CD25 antibody tetramer to selection cocktail or use of EasySep magnetic beads may have increased cell death during costimulation.

We measured cell death on Day 7 of ICAM-1 or CD28 costimulation using flow cytometry with Annexin V and 7AAD staining. Our preliminary results (n=1) suggested that for ICAM-1 costimulation, there was 7.7% dead cells (Annexin V^+ $7AAD^+$) for the standard isolation using StemSep antibody selection cocktail and StemSep magnetic beads; however, for StemSep selection cocktail + CD25 antibody tetramer with StemSep beads there was 17.3% dead cells, and for isolation with StemSep cocktail and EasySep beads there was 35.6% dead cells (**Figure 3.7**, top row). Likewise, for CD28 costimulation, there was 3.5% dead cells for the standard StemSep isolation; however, for StemSep selection cocktail + CD25 antibody tetramer with StemSep beads there was 15.1% dead cells, and for isolation with StemSep cocktail and EasySep beads there was 25.5% dead cells (**Figure 3.7**, bottom row).

Figure 3.7

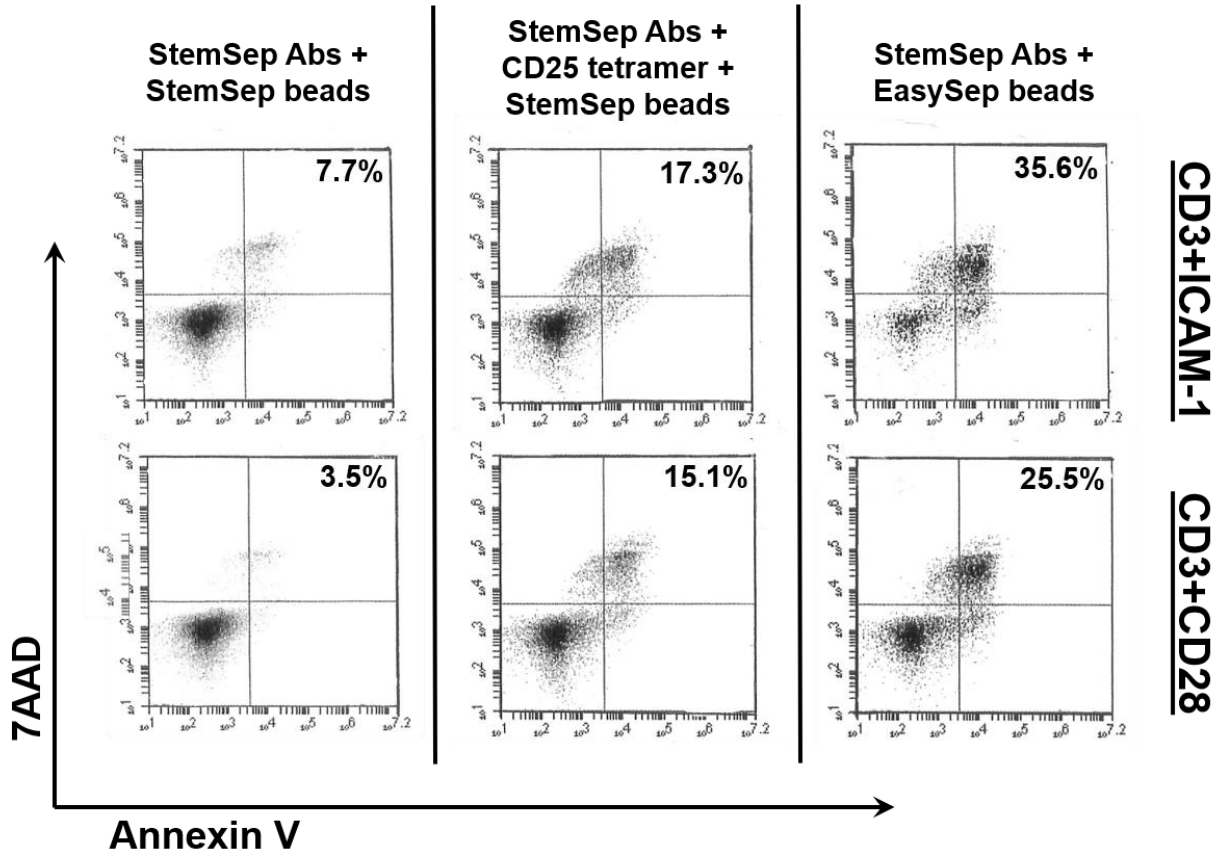
StemSep Abs +
StemSep beads
StemSep Abs +
CD25 tetramer +
StemSep beads
StemSep Abs +
EasySep beads
7.7%
17.3%
35.6%
3.5%
15.1%
25.5%
CD3+ICAM-1
CD3+CD28
7AAD
Annexin V

Figure 3.7 Addition of CD25 antibody tetramer to negative selection cocktail or use of EasySep beads increased cell death. Naïve T cells were purified from peripheral blood using StemSep antibody cocktail with StemSep magnetic beads (left), StemSep antibody cocktail with CD25 tetramer and StemSep magnetic beads (center), or StemSep antibody cocktail with EasySep magnetic beads (right). Naïve T cells from each isolation were stimulated through CD3+ICAM-1 (top row) or CD3+CD28 (bottom row) for 7 days before analysis by flow cytometry. Percentage of dead cells is shown in the UR (Annexin V^+ $7AAD^+$) quadrant in bold; n=1.

Discussion

We have used StemSep human naïve $CD4^+$ T cell negative selection kits to isolate functional cells from peripheral blood for more than 15 years. As we have previously demonstrated (references 18-20 as well as the dissertations of Drs. Jake Kohlmeier, Kelli Williams, Abby Dotson, and Amy Newton), naïve T cells isolated in this way activate, proliferate, differentiate into effector and memory cells of various T cell subsets, and produce cytokines in response to costimulation through CD28, ICAM-1, LFA-1, and CTLA-4 without addition of exogenous cytokines. However, StemCell discontinued this kit and replaced it with EasySep, which is different from the StemSep kit in that it is column-free, employs a selection cocktail with antibodies against several additional cell targets, and utilizes larger magnetic beads.

We compared the StemSep and EasySep kits by performing differentiation experiments using cells isolated from the same blood donor. Our initial finding was that yields of naïve $CD4^+$ T cells were reduced for EasySep isolations even though the number of PBMC obtained per donor for each experiment was comparable as was the purity of the resulting naïve cells. This reduction in cell yield was unsurprising. With the additional selection antibodies in EasySep, one would expect more cells to be targeted for removal.

We observed less activation (indicated by cell clumping during microscopic observation) during costimulation and fewer blasts, with an increase in the dead cell population for EasySep. In agreement with these findings, there was also a large increase in cell death and reduced effector and memory cell differentiation for both costimulations in the EasySep naïve cells.

Naïve T cells isolated using EasySep did not differentiate comparably during costimulation and a large percentage of these cells were dead by Day 7. We hypothesized that the additional selection antibodies in EasySep may remove a subset of naïve T cells which are essential for differentiation and cell survival or that some component of EasySep is toxic to naïve T cells. Naïve T cells are a relatively recently discovered population of cells, the properties and surface markers of which are still being elucidated, so it is possible that one of the selection antibodies that was intended to target a non-naïve cell for removal instead binds to a naïve cell and removes it, since expression of that particular protein had not yet been determined for naïve T cells.

The selection cocktail of EasySep contains CD25 antibody tetramer, while the StemSep cocktail does not. CD25 is the IL-2 receptor α chain, and IL-2 is a critical T cell cytokine promoting growth and differentiation. Recent work indicates CD25 is weakly expressed on naïve T cells (4-5). Therefore, it is possible that the CD25 tetramer could remove the $CD25^{+}$ population of naïve T cells. Further, removing this population of cells capable of responding to IL-2 could potentially perturb naïve T cell differentiation. Further, our in vitro differentiation system, which relies on stimulation of cell surface receptors by antibodies instead of exogenous cytokines, may be particularly vulnerable to detrimental effects caused by loss of the $CD25^{+}$ population. Our preliminary results suggested that removal of the $CD25^{+}$ population of naïve T cells inhibited effector cell differentiation and promoted cell death. This result also suggested a significant role for CD25/IL-2 in naïve T cell differentiation, even for naïve T cells that are $CD25^{(-)}$.

The only published differences between the StemSep magnetic beads and the EasySep magnetic beads are their sizes (50-100 nm diameter for StemSep versus 150-450 nm for

EasySep) and the solution in which they are suspended (saline for StemSep versus sterile water for EasySep). As such, we thought it unlikely that the magnetic beads themselves would make a noticeable difference in differentiation outcome but, in the interest of thoroughness, decided to test this assumption. Our initial assay found that differentiation of effector cells was greatly reduced and cell death was increased for naïve T cells isolated using the StemSep selection cocktail and the EasySep beads compared to naïve T cells isolated using StemSep cocktail and StemSep beads.

This result was surprising because the beads themselves are not intended to directly interact with the naïve T cells since the isolation is based on negative selection. Further, the cell suspension was only incubated with the magnetic beads for 15 minutes. Observing marked differences in effector cell number and dead cell number 7 days later was therefore unexpected. We hypothesize that there may have been additional components of the magnetic bead suspension beyond water and the beads that were proprietary and are somewhat toxic to naïve T cells.

We observed that naïve $CD4^+$ T cells isolated using EasySep did not activate or differentiate comparably to those isolated using StemSep. Additionally, inclusion of CD25 antibody tetramer in the EasySep selection cocktail as well as the EasySep magnetic beads both may have played a role in the loss of differentiation but neither component was fully responsible for the observed differences in the EasySep naïve T cells.

Chapter 3. References

1. S. Woodside and T. Thomas, inventors. Magnetic cell separation method. US patent 2000024824. 2 February 2006.
2. R. L. Mohrmann and D. A. Arber, 2000, CD20-positive peripheral T-cell lymphoma: Report of a case after nodular sclerosis Hodgkin's disease and review of the literature. *Mod Pathol* 13: 1244-1252.
3. E. Schuh, K. Berer, M. Mulazzani, K. Feil, I. Meinl, H. Lahm, M. Krane, R. Lange, K. Pfannes, M. Subklewe, R. Gürkov, M. Bradl, R. Hohlfeld, T. Kümpfel, E. Meinl and M. Krumbholz, 2016, Features of human CD3+CD20+ T cells. *J Immunol* 197: 1111.
4. C. A. Dendrou, V. Plagnol, E. Fung, J. H. M. Yang, K. Downes, J. D. Cooper, S. Nutland, G. Coleman, M. Himsworth, M. Hardy, O. Burren, B. Healy, N. M. Walker, K. Koch, W. H. Ouwehand, J. R. Bradley, N. J. Wareham, J. A. Todd and L. S. Wicker, 2009, Cell-specific protein phenotypes for the autoimmune locus *IL2RA* using a genotype-selectable human bioresource. *Nat Genet* 41: 1011-1015.
5. M. L. Pekalski, R. C. Ferreira, R. M. R. Coulson, A. J. Cutler, H. Guo, D. J. Smyth, K. Downes, C. A. Dendrou, X. Castro Dopico, L. Esposito, G. Coleman, H. E. Stevens, S. Nutland, N. M. Walker, C. Guy, D. B. Dunger, C. Wallace, T. I. M. Tree, J. A. Todd and L. S. Wicker, 2013, Postthymic expansion in human CD4 naive T cells defined by expression of functional high-affinity IL-2 receptors. *J Immunol* 190: 2554-2566.
6. R. L. Silverstein and M. Febbraio, 2009, CD36, a scavenger receptor involved in immunity, metabolism, angiogenesis, and behavior. *Sci Signal* 2: re3.
7. E. A. Podrez, M. Febbraio, N. Sheibani, D. Schmitt, R. L. Silverstein, D. P. Hajjar, P. A. Cohen, W. A. Frazier, H. F. Hoff and S. L. Hazen, 2000, Macrophage scavenger receptor

CD36 is the major receptor for LDL modified by monocyte-generated reactive nitrogen species. *J Clin Invest* 105: 1095-1108.

8. E. A. Podrez, E. Poliakov, Z. Shen, R. Zhang, Y. Deng, M. Sun, P. J. Finton, L. Shan, M. Febbraio, D. P. Hajjar, R. L. Silverstein, H. F. Hoff, R. G. Salomon and S. L. Hazen, 2002, A novel family of atherogenic oxidized phospholipids promotes macrophage foam cell formation via the scavenger receptor CD36 and is enriched in atherosclerotic lesions. *J Biol Chem* 277: 38517-38523.
9. D. M. Knowles, B. Tolidjian, C. Marboe, V. Agati, M. Grimes and L. Chess, 1984, Monoclonal anti-human monocyte antibodies OKM1 and OKM5 possess distinctive tissue distributions including differential reactivity with vascular endothelium. *J Immunol* 132: 2170.
10. C. Arce, A. Moreno, J. M. Perez de la Lastra, J. J. Garrido, M. Barbancho, D. F. De Andres, L. Morera and D. Llanes, 2001, Expression of CD61 (beta3 integrin subunit) on canine cells. *Platelets* 12: 69-73.
11. J. Yoon, A. Terada and H. Kita, 2007, CD66b regulates adhesion and activation of human eosinophils. *J Immunol* 179: 8454-8462.
12. W. Du, J. Li, W. Liu, Y. He, J. Yao, Y. Liu, J. Lin and J. Zheng, 2016, Interleukin-3 receptor alpha chain (CD123) is preferentially expressed in immature T-ALL and may not associate with outcomes of chemotherapy. *Tumour Biol* 37: 3817-3821.
13. K. Renner, S. Metz, A. M. Metzger, S. Neumayer, K. Schmidbauer, Y. Talke, S. Buchtler, D. Halbritter and M. Mack, 2018, Expression of IL-3 receptors and impact of IL-3 on human T and B cells. *Cell Immunol* 334: 49-60.

14. A. L. Revenfeld, R. Steffensen, L. H. Pugholm, M. M. Jorgensen, A. Stensballe and K. Varming, 2016, Presence of HLA-DR molecules and HLA-DRB1 mRNA in circulating CD4(+) T cells. *Scand J Immunol* 84: 211-221.
15. Mark M. Davis and Yueh-Hsiu Chien, 2008. T cell antigen receptors. In *Fundamental Immunology*, 6th ed. W. E. Paul, ed. Wolters Kluwer Health: Lippincott Williams & Wilkins, Philadelphia, PA. p. 313-345.
16. J. E. Kohlmeier, L. M. Rumsey, M. A. Chan and S. H. Benedict, 2003, The outcome of T-cell costimulation through intercellular adhesion molecule-1 differs from costimulation through leucocyte function-associated antigen-1. *Immunology* 108: 152-157.
17. S. A. Tibbetts, C. Chirathaworn, M. Nakashima, D. S. Jois, T. J. Siahaan, M. A. Chan and S. H. Benedict, 1999, Peptides derived from ICAM-1 and LFA-1 modulate T cell adhesion and immune function in a mixed lymphocyte culture. *Transplantation* 68: 685-692.
18. A. H. Newton and S. H. Benedict, 2014, Low density lipoprotein promotes human naive T cell differentiation to Th1 cells. *Hum Immunol* 75: 621-628.
19. K. M. Williams, A. L. Dotson, A. R. Otto, J. E. Kohlmeier and S. H. Benedict, 2011, Choice of resident costimulatory molecule can influence cell fate in human naive CD4+ T cell differentiation. *Cell Immunol* 271: 418-427.
20. J. E. Kohlmeier, M. A. Chan and S. H. Benedict, 2006, Costimulation of naive human CD4 T cells through intercellular adhesion molecule-1 promotes differentiation to a memory phenotype that is not strictly the result of multiple rounds of cell division. *Immunology* 118: 549-558.

Chapter 4. Summary: Development and testing peptides corresponding to ICAM-1 and LFA-1 as a potential therapy for equine recurrent uveitis

This project was undertaken as a collaboration with Dr. Abby Dotson and Dr. Susan Keil, veterinary ophthalmologist.

Equine recurrent uveitis (ERU) is a progressive inflammatory disease of the eye which affects 15% of horses and can lead to blindness. ERU has many characteristics of autoimmune disease. Current therapies for autoimmune conditions are generally immunosuppressive, blocking the activation of not only self-reactive immune cells but also immune cells that protect the organism from infection. Our lab has previously developed therapeutic peptides corresponding to the contact domains of ICAM-1 and LFA-1, inhibiting the interaction of these two receptors and inactivating only self-reactive immune cells and leaving normal, protective immune cells fully functioning. We have demonstrated the efficacy of these peptides in blocking human T cell activation during in vitro mixed lymphocyte reactions (MLRs) as well as protecting against autoimmune disease in murine models of rheumatoid arthritis and emphysema.

Here, we designed cyclic peptides corresponding to the equine sequences of ICAM-1 and LFA-1. We demonstrated the ability of these peptides to dose-dependently inhibit activation of equine T cells measured by homotypic adhesion assays using mitogen-treated total T cells purified from the peripheral blood of healthy horses as well as horses with ERU. Next, we measured proliferation of equine T cells treated with peptides during MLR. Surprisingly, we observed that T cell proliferation dose-dependently increased during treatment with both ICAM-1 and LFA-1 peptides together. Further studies suggested that treatment with the equine ICAM-1

peptide alone promoted T cell proliferation beyond that induced by phytohemagglutinin, but treatment with the equine LFA-1 peptide did not affect proliferation.

This suggested that the ICAM-1 peptide was somehow stimulating the T cells, potentially by interacting with cell surface ICAM-1. These data suggested that the equine ICAM-1 peptide would not be useful as a therapy for autoimmunity but the peptide may have other potential uses. Further, redesign of this peptide could remove its stimulatory ability, allowing its potential use for treatment of autoimmunity.

We also attempted to develop an antigen recall assay that could potentially be used to help diagnose ERU. In this assay, peripheral blood mononuclear cells (PBMCs) from a horse suspected of having ERU would be treated with an equine eye-specific protein and proliferation response to this antigen would be evaluated. Cells from horses that had ERU would be expected to proliferate in response to eye antigen, while cells from healthy horses would not proliferate. We tested several antigens on PBMCs from both healthy and ERU horses but proliferation was comparable to the unstimulated control for all antigens at all concentrations tested. One potential explanation for the failure of the antigens to stimulate equine cells could be that the eye antigens were purified human proteins, since there were no commercially available equine proteins available at the time. It is possible that the human antigens were dissimilar enough from the equine antigens that they failed to elicit a response from the equine immune cells.

Another alternative is that there were insufficient antigen-presenting cells in our PBMCs. We had purified PBMCs from equine blood using a standard density gradient centrifugation protocol with standard Ficoll of 1.077 g/ml density (optimal density for human PBMC isolation). However, immediate post-isolation staining of the PBMCs for CD3, the T cell receptor, showed

that the PBMCs were 95-98% $CD3^+$, suggesting an unusually low percentage of antigen-presenting cells for a PBMC preparation. A not-inconsiderable quantity of literature searching indicated that the optimal density of the density centrifugation reagent was 1.068 g/ml for equine PBMCs. The next step towards developing the ERU antigen recall assay would be to isolate PBMCs using 1.068 g/ml density Ficoll as well as testing purified equine ocular antigens instead of human or another species.

Chapter 5. Summary: Associated proteins of the ICAM-1 signaling complex in human T cells and comparison with the CD28 signaling complex

Previous work in our laboratory by Dr. Chintana Chirathaworn and Dr. Jake Kohlmeier demonstrated that stimulating T cells through ICAM-1 induces phosphorylation of several proteins and can serve as a second signal for T cell activation and differentiation. Costimulation of human naïve $CD4^+$ T cells through ICAM-1 promotes differentiation into T helper 1 and T regulatory cells but not T helper 2 cells, while costimulation through CD28 promotes differentiation into T helper 1 and T helper 2 cells but not T regulatory cells. These alternative differentiation outcomes imply that the signaling induced by ICAM-1 stimulation is not the same as the signaling induced by CD28 stimulation. This work is part of a long term, ongoing effort by our laboratory to understand ICAM-1 signaling in T cells.

Dr. Chirathaworn showed that in Molt3, an ICAM-1^+ T cell leukemia, ICAM-1 crosslinking induced association with cdc2 and Lck kinases and also showed a constitutive association with ERK2. Her data also supported induced phosphorylation of cdc2 on ICAM-1 crosslinking which correlated with inactivation of cdc2. Preliminary data from Dr. Brian Wick indicated that ERK2 may be phosphorylated on ICAM-1 stimulation

We verified the surface expression of ICAM-1 on Molt3 T cells by flow cytometry. We also confirmed the work of Drs. Chirathaworn, Williams, and Wick in human T cell lines and primary T cells using co-immunoprecipitation assays. We demonstrated that ZAP-70 kinase became associated with ICAM-1 after 2 minutes of stimulation and leaving the complex by 6

minutes. We also found that the related Syk kinase may also be inducibly associated with ICAM-1, which agrees with the work of other investigators in other non-immune cell types.

Our preliminary data indicated that ZAP-70 did not associate with CD28 on stimulation, unlike ICAM-1 stimulation. We also examined the association of ERK1/2 with CD28. We showed that ERK1/2 became associated with CD28 at 2-10 minutes of stimulation. Conversely, ERK2 only was constitutively associated with ICAM-1. Lck may be associated with CD28 at 2 minutes of stimulation and then leaving the complex, similar to the kinetics of the association of Lck with ICAM-1.

We demonstrated that the ICAM-1 signaling complex in human T cells contains ZAP-70 and Syk while the CD28 complex includes Lck and ERK1/2 but not ZAP-70.

Chapter 6. Summary: Preliminary data comparing the ICAM-1 signaling protein complex in mouse and human T cells

Our lab has previously demonstrated that costimulation of human naïve $CD4^+$ T cells through ICAM-1 promotes differentiation of T regulatory cells without addition of exogenous cytokines. The laboratory has previously patented an autologous T cell therapy for treatment of autoimmune disease based on this observation, in which naïve $CD4^+$ T cells would be purified from the patient's blood, costimulated through ICAM-1 to induce T regulatory cell differentiation, and then returned to the patient. Once the T regulatory cells have been reintroduced to the patient, they would circulate the body suppressing autoimmune inflammation. This therapy offers a significant advantage over current therapies for autoimmune conditions, which are globally immunosuppressive, leaving the patient vulnerable to infection. However, our proposed autologous T cell therapy would shut down autoimmune inflammation but leave the patient's immune system able to respond appropriately to exogenous threats. The next step towards developing this idea as a therapy would entail a demonstration of its efficacy in a mouse model of autoimmunity. However, previous lab members have shown that murine T cells do not differentiate into T regulatory cells during ICAM-1 costimulation. As such, it was of interest to determine how the murine ICAM-1 signaling pathway diverges from the human pathway.

Due to the difficulty in obtaining primary mouse T cells in sufficient quantity for the proposed coimmunoprecipitation studies, we chose to use EL4, a murine T cell lymphoma. We first characterized our EL4 line using flow cytometry, showing that the cells were $CD3^+$ $CD4^+$

CD11a^{+} ICAM-1^{+}. Next, we verified the kinetics and ability of the mouse anti-ICAM-1 antibody to stimulate EL4 cells by crosslinking with a secondary antibody, finding that ICAM-1 stimulation induced alterations in tyrosine phosphorylation of several proteins via western blot and induced increase in CD69 expression (a marker of T cell activation) over time by flow cytometry. Therefore, we concluded that our ICAM-1 antibody was inducing signaling events in the mouse T cells. Next, we titrated the ICAM-1 antibody to optimize conditions for ICAM-1 immunoprecipitation.

Finally, we used ICAM-1 co-immunoprecipitation to look for proteins which associated with ICAM-1 during stimulation. Preliminary data suggested that Lck was inducibly associated with ICAM-1 upon stimulation, similar to our lab's observations in human T cells. Likewise, cdc2 was associated with ICAM-1 at 2 minutes of stimulation then leaving the complex, as in human T cells. In contrast to our findings concerning the human ICAM-1 complex, in the murine ICAM-1 complex ZAP-70 was not present at any time point; nor were ERK1/2.

These preliminary results support our hypothesis that ICAM-1 signaling is different in mouse and human T cells.